

# Satellite Constellation Design Methodology for Optimal Regional Coverage

Hang Woon Lee\*

*Georgia Institute of Technology, Atlanta, GA, 30332*

Seiichi Shimizu<sup>†</sup>, Shoji Yoshikawa<sup>‡</sup>

*Mitsubishi Electric Corporation, Amagasaki, Japan*

Koki Ho<sup>§</sup>

*Georgia Institute of Technology, Atlanta, GA, 30332*

The use of regional coverage satellite constellations is on the rise urging the need for an optimal constellation design method for complex regional coverage. Traditional constellations are often designed for global coverage; however, the few existing regional constellation design methods lead to a suboptimal solution for disjoint or time-varying regional coverage. This paper introduces a new general and computationally efficient method to design an optimal regional coverage satellite constellation system that satisfies the general coverage requirement that can be disjoint and time-varying. The circular convolution nature of the repeating ground track orbit and common ground track constellation is formalized. This formulation of the constellation configuration architecture allows linearity in the problem formulation, i.e., multiple target areas and multiple sub-constellations with different orbital characteristics can be simultaneously optimized. Two methods are developed herein based on this fundamental relationship, While-Loop and Binary Integer Programming, aiming to optimally design a constellation with the smallest number of satellites possible. An analysis shows that the While-Loop method provides a computationally efficient approximation, whereas the Binary Integer Programming method yields optimal solutions. Seven comprehensive illustrative examples are analyzed to demonstrate the value provided by the proposed approach.

## Nomenclature

- $a$  = semi-major axis  
 $b$  = coverage timeline  
 $c$  = coverage satisfactory indicator over a target point

\*Ph.D. Student and National Science Foundation Graduate Research Fellow, Daniel Guggenheim School of Aerospace Engineering.

<sup>†</sup>Researcher, Mechatronics Department, Advanced Technology R&D Center.

<sup>‡</sup>Chief Researcher, Mechatronics Department, Advanced Technology R&D Center.

<sup>§</sup>Assistant Professor, Daniel Guggenheim School of Aerospace Engineering. Member AIAA.

$C$	=	coverage satisfactory indicator over an area of interest
$d$	=	satellite constellation architecture design vector
$e$	=	eccentricity
$F$	=	phasing factor (Walker notation)
$f$	=	coverage requirement vector
$i$	=	inclination
$\mathcal{J}$	=	set of target point(s)
$L$	=	length (period) of vectors
$m$	=	dummy index for convolution
$M$	=	mean anomaly
$n$	=	discrete-time instant
$N$	=	total number of satellites
$N_D$	=	number of sidereal days
$N_P$	=	number of revolutions
$p$	=	semi-latus rectum
$P$	=	number of orbital planes (Walker notation)
$P_\pi$	=	permutation matrix
$q$	=	generalized index
$r_g$	=	target point position vector
$r_s$	=	satellite position vector
$R_E$	=	mean radius of the Earth
$t$	=	continuous-time instant
$t_{step}$	=	sampling rate
$T_G$	=	nodal period of Greenwich
$T_S$	=	nodal period of the satellite
$v$	=	access profile
$V$	=	access profile circulant matrix
$x$	=	constellation pattern vector
$X$	=	constellation pattern vector circulant matrix
$\mathcal{Z}$	=	set of sub-constellation(s)
$\mathbb{Z}_2$	=	binary integer number set
$\mathbb{Z}_{>0}$	=	positive integer number set

- $\mathbb{Z}_{\geq 0}$  = non-negative integer number set  
 $\alpha$  = row entry index  
 $\beta$  = column entry index  
 $\delta$  = satellite spacing constant  
 $\varepsilon$  = elevation angle  
 $\varepsilon_{min}$  = minimum elevation angle  
 $\lambda$  = latitude  
 $\mu_E$  = standard gravitational parameter of the Earth  
 $\rho$  = relative position vector from target point to satellite  
 $\tau$  = period ratio  
 $\phi$  = longitude  
 $\omega$  = argument of perigee  
 $\omega_E$  = rotation rate of the Earth  
 $\Omega$  = right ascension of ascending node  
 $\mathbf{e}$  = orbital element vector
- Subscripts
- $j$  = target point index  
 $k$  = satellite index
- Superscripts
- $z$  = sub-constellation index

## I. Introduction

Satellite constellation for regional coverage is increasingly being considered as a competent business solution in the market dominant of global-based constellation systems. Regional constellation, whose form varies from being standalone to augmenting existing space-borne systems, provides flexible solutions to stakeholders as a means of circumventing geopolitical, economic, and/or technical issues associated with global constellation systems. Examples of such regional constellation systems are the BeiDou Navigation Satellite System [1], Indian Regional Navigation Satellite System (IRNSS) [2], and Quasi-Zenith Satellite System [3].

Unlike global coverage constellations, regional coverage constellations solely focus on the coverage over a local region and therefore generally require a smaller number of satellites in the system to achieve the same performance per area metric compared to the global-coverage constellations. This leads to a significantly reduced system cost as the total life-cycle cost of the system depends on the number of satellites [4]. The reduced system cost allows for a tolerable risk

of failure and facilitates a shorter payback period. These properties allow regional constellation systems to swiftly react to uncertainties arising from market demand and/or administrative issues. A study has shown that a flexible option to treat a regional constellation system as a part of a larger staged deployment process can be beneficial when market uncertainties are present [5].

Various space systems have been designed for regional coverage. The most classical example is to use Geosynchronous/-stationary equatorial (GSO/GEO) orbits, which has proven to be very effective for continuous coverage over a bounded local region. However, for many mission-critical attributes such as latency and launch cost, non-geostationary orbit (NGSO) systems are deemed to provide better performance. The design process to generate a constellation specifically for regional coverage utilizing non-geostationary satellite orbits is highly complex and scarcely studied in the literature. Furthermore, while traditional methods have looked into the problem of  $f$ -fold continuous coverage (e.g., single fold, double fold, etc.) or intermittent coverage with figures of merit such as the maximum revisit time, the problem of much more complex time-varying coverage over multiple targets (e.g., a system that simultaneously provides single fold coverage over area A and double fold coverage over area B) has not been explored. Such a regional coverage constellation system can constitute multiple sub-constellations, each with different orbital characteristics [6]. The concurrent optimization of multiple sub-constellations in the system is also scarcely studied. Based on this background, a research question of interest arises: “*Can we design a system of multiple sub-constellations that is solely optimized for a regional area of interest where the optimality is driven by the number of satellites? If so, how do we design it?*” This paper seeks to address this question by constructing a constellation design methodology specialized for regional coverage.

The contribution of this paper is as follows: First, a discovery of *circular convolution phenomenon* between seed satellite access profile, constellation pattern vector, and coverage timeline is formalized. We derive a linear formulation that enables us to design a system of multiple sub-constellations for multiple regions, which provides a foundation for general and computationally efficient methods introduced herein. Second, we develop a While-Loop method that assumes symmetry in satellite configuration and enables computational efficient approximation to be used in large optimization settings. Third, inspired by the idea of deconvolution, we develop a method based on Binary Integer Programming that find the optimal satellite constellation configuration for regional coverage. This core concept enables users to explore the hidden design space by breaking the symmetry in the constellation design. Finally, we extend the traditional definition of a time-independent  $f$ -fold coverage requirement (e.g., single-fold, double-fold, etc.) to time-dependent  $f[n]$ -fold coverage requirement, where  $n$  is the discrete-time instant (e.g., diurnal variations in coverage requirement), so that time-varying coverage demands can be handled optimally in constellation design.

The rest of the paper is organized as follows. Section II provides a summary of key relevant literature. Section III provides an overview of assumptions made in this paper. Section IV introduces the circular convolution formulation of the problem and its pertinent definitions. Section V then derives two methods based on this formulation: While-Loop

and Binary Integer Programming. These methods are then demonstrated in Section VI with various illustrative examples. Section VII then concludes this paper.

## II. Literature Review

This section reviews the major literature relevant to this study. Traditional satellite constellation design methods have focused on minimizing the number of satellites while providing continuous coverage over a large area of interest such as the globe or latitudinally-bounded zones. Classical methods such as the streets of coverage [7–10], Walker constellations [11–14], and the tetrahedron elliptical constellation [15] leveraged geometric approach to exhibit symmetry in the constellation pattern, where satellites are uniformly and symmetrically arranged based on a predetermined phasing rule. The symmetry in the constellation pattern provides a foundation for a complete design space analysis due to finite variability [16] or for an analytical solution. Nonetheless, this usually leads to redundant coverage overlaps and therefore may not produce an optimal constellation design in terms of the number of satellites.

There are several prior studies that specifically deal with the regional coverage constellation design, particularly leveraging the repeating ground track orbits (e.g., Flower Constellation set theory [17–19]). By fully utilizing the characteristics of the repeating ground track orbits, Hanson et al. and Ma and Hsu utilized the timeline meshing method to generate the optimal constellation with respect to minimizing the gap [20, 21]. Similarly, Pontani and Teofilatto extended the characteristics of the repeating ground track by searching for allowable time delays with respect to minimizing the gap or maximizing coverage [22]. Although these regional constellation design algorithms show promising ability to produce asymmetric configuration with respect to a single target point, these methods are not applicable for designing a constellation system with respect to multiple target points and time-varying demands with multiple sub-constellations. Ulybyshev investigated a new geometric approach to generate satellite constellation designs for complex coverage [23]. Nevertheless, this method cannot be applied to an asymmetric constellation such as a near-polar constellation as noted by the author. Researchers utilized heuristic algorithms, such as genetic algorithm and simulated annealing, to design satellite constellations for regional coverage [24, 25]. However, consideration of multiple sub-constellations have been neglected. Other literature can be found in the comprehensive literature review by Dutruel-Lecohier and Mora as well as Wertz and Larson [26, 27]. Recently, Ulybyshev presented a short historical survey of satellite constellation design for continuous coverage [28]. However, there is no methodology that directly answers our question raised in the introduction that considers all three aspects of the regional coverage problem: (1) multiple target points, (2) time-varying coverage requirement, and (3) multiple sub-constellations.

In response to this background, this paper attempts to construct a general regional coverage satellite constellation design method that is capable of designing a regional constellation system of multiple sub-constellations that satisfies the complex coverage requirements of multiple target points with the minimum number of satellites possible by breaking the symmetry in the constellation pattern. The complex coverage requirement here refers to of any type—continuous,

intermittent, time-varying, etc.—that can be represented in a non-negative integer form.

### III. Satellite Constellation Generation

#### A. Repeating Ground Track Orbit

A ground track of a satellite is defined as a trace of its sub-satellite points on the surface of the Earth. In this paper, we utilize a repeating ground track (RGT) orbit as a basis for the orbital design of the constellation, which allows a ground track of a satellite to repeat exactly and periodically. This type of orbit has shown to provide better coverage performance than the non-repeating ground track orbits with a fewer number of satellites for regional coverage [20]. Considering the Earth-centered Earth-fixed (ECEF) frame, an RGT orbit is achieved when the nodal period of the orbit  $T_S$  is matched with the nodal period of Greenwich  $T_G$  [17]:

$$N_P T_S = N_D T_G \quad (1)$$

where a satellite makes  $N_P$  number of revolutions in  $N_D$  number of sidereal days.

A period ratio  $\tau$  is defined as a ratio of  $N_P/N_D$  and further can be deduced based on the perturbed orbital elements.

$$\tau = \frac{N_P}{N_D} = \frac{T_G}{T_S} = \frac{\dot{\omega} + \dot{M}}{\omega_E - \dot{\Omega}} \quad (2)$$

where  $\omega_E$  is the rotation rate of the Earth,  $\dot{\omega}$  is the rate of the apsidal precession,  $\dot{\Omega}$  is the rate of nodal regression of a satellite's orbit, and  $\dot{M}$  is the rate of change of the mean anomaly due to nominal motion and perturbation. The perturbed orbital elements in Eq. (2) are:

$$\dot{\omega} = \frac{3}{2} J_2 \left( \frac{R_E}{p} \right)^2 \sqrt{\frac{\mu_E}{a^3}} \left[ 2 - \frac{5}{2} \sin^2 i \right] \quad (3)$$

$$\dot{\Omega} = -\frac{3}{2} J_2 \left( \frac{R_E}{p} \right)^2 \sqrt{\frac{\mu_E}{a^3}} \cos i \quad (4)$$

$$\dot{M} = \sqrt{\frac{\mu_E}{a^3}} \left[ 1 - \frac{3}{2} J_2 \left( \frac{R_E}{p} \right)^2 \sqrt{1 - e^2} \left( \frac{3}{2} \sin^2 i - 1 \right) \right] \quad (5)$$

where  $R_E = 6378.137$  km is the mean radius of the Earth,  $p = a(1 - e^2)$  is the semi-latus rectum,  $\mu_E = 398\,600.4418$  km<sup>3</sup>sec<sup>-2</sup> is the standard gravitational parameter of the Earth, and  $J_2 = 0.00108263$  is the zonal harmonic coefficient due to the equatorial bulge of the Earth [16].

Considering up to the  $J_2$  perturbation effect, the semi-major axis  $a$  of an RGT orbit can be derived using the Newton-Raphson method presented by Bruccoleri for a given set of  $N_P$ ,  $N_D$ ,  $e$ , and  $i$  [29]. Because the semi-major

axis is a function of  $\tau$ ,  $e$ , and  $i$ , i.e.,  $a = a(\tau, e, i)$ , we shall utilize the period ratio  $\tau = N_P/N_D$  as an independent orbital variable instead of the semi-major axis  $a$ . Henceforth, this paper utilizes an RGT orbital elements vector,  $\mathbf{\alpha} = [\tau, e, i, \omega, \Omega, M]^T$ , to fully define an RGT orbit of a satellite. We assume the utilization of satellite maneuvers to correct and maintain identical ground track throughout the satellite lifetime, negating the perturbation effects other than the  $J_2$  effect. Note that the right ascension of the ascending node (RAAN)  $\Omega$  and the mean anomaly  $M$  in the RGT orbital elements vector indicate initial values referenced to a given epoch.

## B. Common Ground Track Constellation

This paper assumes that all satellites in the constellation are systematically generated such that their ground tracks overlap to create a single common ground track. In this paper, we refer to this type of constellation as a *common ground track constellation*.

A common ground track constellation has its analogous names in many constellation design theories. For example, certain common ground track constellations utilizing circular RGT orbits can be expressed in Walker notation:  $i : N/P/F$  where  $N$  is the total number of satellites in the system,  $P$  is the number of orbital planes, and  $F$  is the phasing factor.

It also has its latest appearance in the original Flower Constellation theory. The Flower Constellation is defined as a set of  $N$  satellites following the same (closed) trajectory with respect to a rotating frame. For this paper, the ECEF frame is considered. The three conditions to construct the Flower Constellation are as follows [30]:

- 1) The orbital period of each satellite is a rational multiple of the period of the rotating frame.
- 2) The semi-major axis  $a$ , eccentricity  $e$ , inclination  $i$ , and argument of perigee  $\omega$  are identical for all the satellite orbits.
- 3) The right ascension of ascending node  $\Omega_k$  and the mean anomaly  $M_k$  of each satellite ( $k = 1, \dots, N$ ) satisfy:

$$N_P \Omega_k + N_D M_k = \text{constant mod } (2\pi) \quad (6)$$

A common ground track constellation with repeating ground track in the ECEF frame is equivalent to the original Flower Constellation theory. Therefore, this paper utilizes the above three conditions of the original Flower constellation set theory as bases for constellation generations.

## IV. Circular Convolution Formulation

### A. Access Profile

The relative position vector  $\boldsymbol{\rho}$  pointing from a ground target point to a satellite is defined as:

$$\boldsymbol{\rho} = \mathbf{r}_s - \mathbf{r}_g \quad (7)$$

where  $\mathbf{r}_s$  is a satellite position vector from the center of the Earth and  $\mathbf{r}_g$  is a target point position vector from the center of the Earth. Fig. 1 illustrates this relationship.

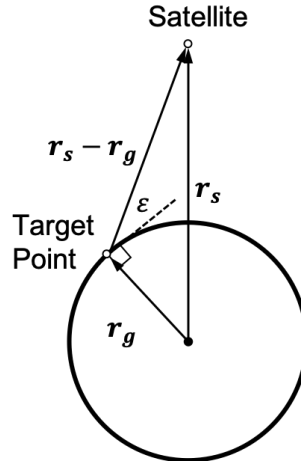


**Fig. 1** Satellite, target point, and elevation angle relationship

An elevation angle  $\varepsilon$  of a satellite seen from a ground target point is defined as:

$$\varepsilon = \sin^{-1} \left( \frac{\mathbf{r}_g \cdot \boldsymbol{\rho}}{\|\mathbf{r}_g\| \|\boldsymbol{\rho}\|} \right) = \sin^{-1}(\hat{r}_g \cdot \hat{\rho}) \quad (8)$$

where  $\|\cdot\|$  is the Euclidean norm.



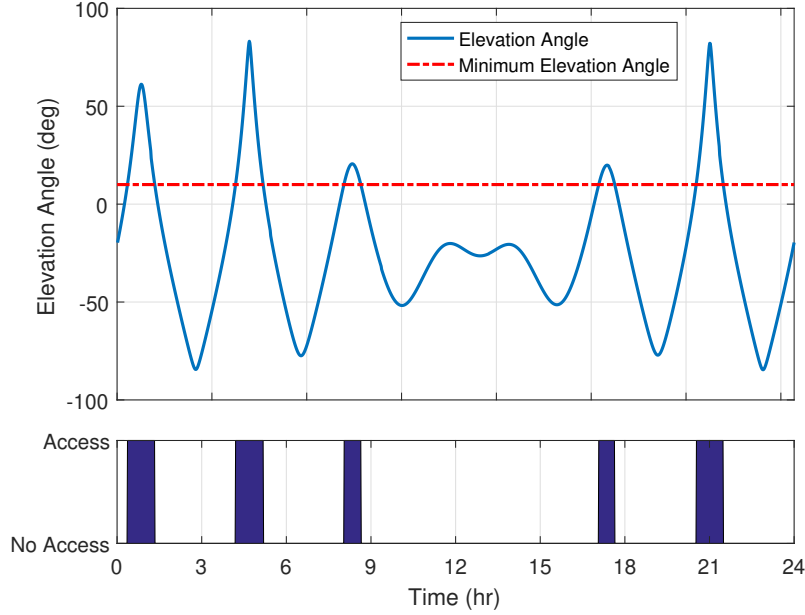


**Fig. 2** Example illustration of a satellite's elevation angle viewed from a ground point and corresponding access profile

Because the dot product between the unit target point position vector  $\hat{r}_g$  and the unit relative position vector  $\hat{\rho}$  continues to change due to the rotation of the Earth and the motion of a satellite, the elevation angle is, therefore, a function of time,  $\varepsilon = \varepsilon(t)$ . An example of a typical NGSO satellite elevation angle function is shown in the top part of Fig. 2. When the elevation angle of a satellite is above the minimum elevation angle threshold  $\varepsilon_{min}$ , which is determined by the mission requirement [31], the satellite is said to be *visible* or *in access with the target point*. Since the periods when the satellite is in access with the ground target point are only of our particular interest, we convert the elevation angle function into the *access profile* (or a visibility profile in some literature), which is a binary vector that indicates either access, 1, or no access, 0, at each time instant  $t$ . The access profile is visualized in the bottom part of Fig. 2. This paper utilizes a sampling method to generate an access profile. Note that access profiles can be derived in many ways [32–34].

The continuous-time elevation angle function  $\varepsilon(t)$  is sampled at every time step of  $t_{step}$  to create a discrete-time elevation angle function  $\varepsilon[n]$  with length  $L$  (i.e., the number of time steps). The access profile  $v_{k,j} \in \mathbb{Z}_2^{L \times 1}$  between the  $k$ th satellite and the  $j$ th target point stores a boolean information of satellite access (or visibility) state at each discrete-time instant  $n$ . Therefore, each element of the access profile is:

$$v_{k,j}[n] = \begin{cases} 1 & \text{if } \varepsilon_{k,j}[n] \geq \varepsilon_{k,j,min}[n] \\ 0 & \text{otherwise} \end{cases} \quad n \in \{0, \dots, L-1\}, \quad k \in \{1, \dots, N\}, \quad j \in \mathcal{J} \quad (9)$$

where  $n$  is the discrete-time instant and  $\mathcal{J}$  is a set of target points. Throughout this paper, both bold  $\mathbf{v}_{k,j}$  and sequential  $\mathbf{v}_{k,j}[n]$  forms are used interchangeably to denote the vector notation.

It is important to note a condition of Eq. (9): there must exist at least one access interval for a given satellite-target in order for the methods introduced in this paper to function. The methods introduced in the following sections are constructed based on the assumption that the access profile is a non-zero vector. When a target point is not within a swath width of a satellite's ground track, the resulting access profile is a vector of all zeros.

One can interpret the generalized minimum elevation angle  $\varepsilon_{k,j,min}[n]$  in Eq. (9) as the minimum elevation angle threshold imposed on an access between a satellite  $k$  and a target point  $j$  at discrete-time instant  $n$ . This paper assumes that all access between a target point  $j$  and every member satellite in a given constellation are equal. That is, we write the simplified minimum elevation angle threshold as:

$$\varepsilon_{k,j,min}[n] = \varepsilon_{j,min}[n], \quad \forall k \in \{1, \dots, N\}, \quad j \in \mathcal{J}, \quad n \in \{0, \dots, L-1\} \quad (10)$$

When designing a satellite constellation for regional coverage, a constellation must be spatially and temporally referenced relative to the target point and the epoch. A hypothetical satellite that conveys referenced orbital information,  $\mathbf{ae}_0 = [\tau, e, i, \omega, \Omega_0, M_0]^T$ , for the constellation is defined as the *seed satellite* (the term is credited to STK of AGI [35]) and the corresponding  $\mathbf{ae}_0$  as the *seed satellite orbital elements vector*. The actual system satellites, specifically, the satellites that are systematically generated based on the referenced orbital information and the phasing rule, inherit the period ratio, the eccentricity, the inclination, and the argument of perigee from the seed satellite, but they hold independent the right ascension of the ascending node and the initial mean anomaly pairs that are determined by Eq. (6), resulting in the orbital element vector for each satellite of  $\mathbf{ae}_k = [\tau, e, i, \omega, \Omega_k, M_k]^T$  where  $k$  is the index of the satellite. Note that  $\Omega$  and  $M$  are initial values referenced to a given epoch; the subscripts refer to the index of a corresponding satellite.

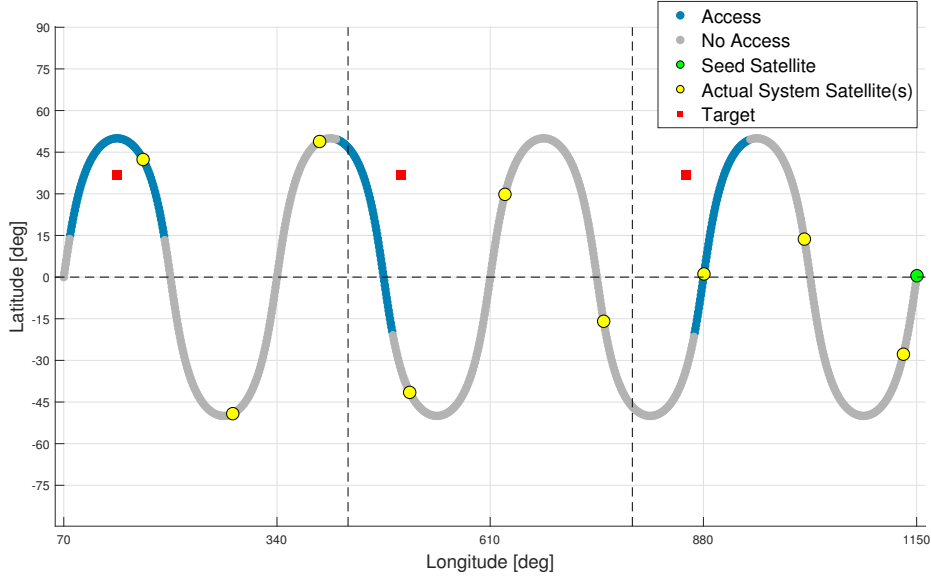


**Fig. 3** Illustration of a common ground track constellation in an expanded ground track view (refer to Appendix A for more information on the expanded ground track view)

Let us recall main assumptions made so far: (1) all satellites are placed on a common repeating ground track constellation as shown in Fig. 3 and (2) all access between a target point  $j$  and every member satellite in a given constellation are constrained to same minimum elevation angle threshold as shown in Eq. (10). Such assumptions enable us to utilize a powerful property, *a cyclic property*, that all access profiles of the member satellites in a given constellation are *identical, but are circularly shifted*. Therefore, any access profile  $v_{k,j}$  between the  $k$ th satellite and the  $j$ th target point can be represented as a circularly shifted *seed satellite access profile*  $v_{0,j}$ :

$$v_{k,j}[n] = P_{\pi}^{nk} v_{0,j}[n], \quad n = \{0, \dots, L - 1\} \quad (11)$$

where  $P_{\pi}$  is a permutation matrix with the dimension  $(L \times L)$  shown in Eq. (35).

For the purpose of this paper utilizing a constellation with a common repeating ground track, the seed satellite access profile  $v_{0,j}$  is of our main interest because of its ability to convey the referenced orbital information.

## B. Coverage Timeline and Coverage Requirement

Because there are multiple satellites in the constellation system, the access profiles must be meshed together to create a *coverage timeline* over a target point. Hence, a coverage timeline  $\mathbf{b}_j \in \mathbb{Z}_{\geq 0}^{L \times 1}$  is an access profile between multiple satellites and a  $j$ th target point. This is illustrated in Fig. 4. In the figure,  $\Delta n_1$  and  $\Delta n_2$  represent discrete time shifts of the first ( $k = 1$ ) and second ( $k = 2$ ) satellite with respect to the seed satellite ( $k = 0$ ), respectively. It is important to point out that because the seed satellite is hypothetical, its access profile is not considered in the coverage timeline.

Note that the coverage timeline is not a binary vector but instead it is a non-negative integer vector. Eq. (12) provides a mathematical definition of the coverage timeline.

$$b_j[n] = \sum_{k=1}^N v_{k,j}[n] \quad (12)$$

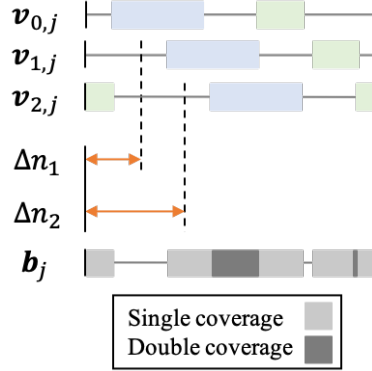


**Fig. 4 Illustration of shifts of access profiles (2-satellite system); notice that the seed satellite access profile is not part of the coverage timeline**

Now we define a *coverage requirement*. A coverage requirement  $f_j \in \mathbb{Z}_{\geq 0}^{L \times 1}$  is a vector of non-negative integers that is created by a user per mission requirement. It is important to distinguish the difference between the coverage timeline  $b_j$  and the coverage requirement  $f_j$ . The coverage timeline is a coverage *performance* or a coverage *state* of a constellation system while the coverage requirement, per se, is a coverage *requirement* a constellation system wants to achieve. For example, in order for a constellation system to achieve the  $f$ -fold (i.e., at least  $f$  satellites in view at all times) continuous coverage, the coverage timeline must be greater than or equal to the coverage requirement, that is, at least  $f$  satellite(s) must be in access with the target point throughout the mission period.

The coverage satisfactoriness indicator  $c_j$  indicates the coverage requirement satisfactoriness of the coverage timeline over the target point  $j$ .

$$c_j = \begin{cases} 1 & \text{if } b_j[n] \geq f_j[n], \forall n = \{0, \dots, L-1\} \\ 0 & \text{otherwise} \end{cases} \quad (13)$$

If an area of interest consists of multiple target points (e.g., due to area grid discretization), the coverage is satisfactory if all target points are satisfactorily covered. Extending Eq. (13), the satisfactory condition of the coverage over multiple targets can be expressed as:

$$C = \begin{cases} 1 & \text{if } c_j = 1, \forall j \in \mathcal{J} \\ 0 & \text{otherwise} \end{cases} \quad (14)$$

where  $\mathcal{J}$  is a set of target points.

In summary, designers of the constellation system must aim to satisfy all coverage requirements on every target point. Each target point may impose a different coverage requirement.

### C. Constellation Pattern Vector

Suppose we express the time shifts of satellites along the ground track with respect to the seed satellite in a discrete-time binary sequence  $\mathbf{x} \in \mathbb{Z}_{\geq 0}^{L \times 1}$  and refer to it as a *constellation pattern vector*.

$$x[n] = \begin{cases} 1 & \text{if satellite exists at time instant } n \\ 0 & \text{otherwise} \end{cases} \quad (15)$$

where we deduce the number of satellites in the constellation from the constellation pattern vector:

$$N = \sum_{n=0}^{L-1} x[n] \quad (16)$$

By definition, a  $k$ th satellite located at time instant  $n_k$  is said to be delayed behind the seed satellite by the time unit of  $\Delta n_k = t_{step} n_k$ . This is illustrated in Fig. 5. The left-hand side of the figure shows a snapshot of the distribution of two satellites—the seed satellite in green and the arbitrary  $k$ th satellite in yellow circles—in an expanded ground track view. The  $k$ th satellite is positioned behind the seed satellite along the moving direction by the time unit of  $\Delta n_k$ . The equivalent representation is shown on the right-hand side of the figure, which represents this physical relationship in the constellation pattern vector form. In this case, the position of the  $k$ th satellite is represented as a red impulse representing the time delay with respect to the seed satellite.

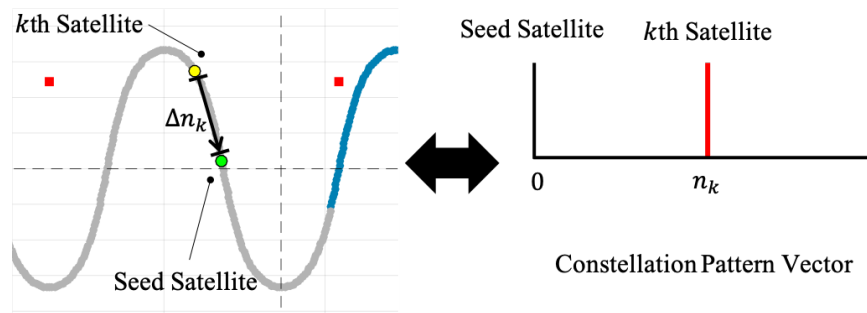


**Fig. 5** Illustration of a satellite time shift and its representation in constellation pattern vector form; the direction of the motion of satellites is indicated by the arrow on the left-hand side of the figure

#### D. The Circular Convolution Phenomenon

The discrete-time sequences defined in the previous sections— $v_{0,j}$ ,  $\mathbf{x}$ , and  $\mathbf{b}_j$ —have a finite periodic length of  $L$  due to the cyclic (repeatability) property of the closed relative ground track assumption.

A discrete circular convolution operation between the seed satellite access profile  $v_{0,j}$  and the constellation pattern vector  $\mathbf{x}$  produces a coverage timeline  $\mathbf{b}_j$ , a timeline of an instantaneous number of satellites in access with the target point:

$$\begin{aligned} b_j[n] &= v_{0,j}[n] \circledast x[n] = \sum_{m=0}^{L-1} v_{0,j}[m]x[(n-m) \bmod L] \\ &= x[n] \circledast v_{0,j}[n] \end{aligned} \quad (17)$$

where  $\circledast$  represents a circular convolution operator. Note that the circular convolution is commutative. The derivation of the circular convolution relationship from Eq. (12) is described in Appendix B.

The discrete-time circular convolution in Eq. (17) can be further expressed in a circulant matrix form.

$$V_{0,j}\mathbf{x} = \mathbf{b}_j \quad (18)$$

where  $V_{0,j} \in \mathbb{Z}_2^{L \times L}$  is a seed satellite access profile circulant matrix that is fully specified by the seed satellite access profile  $v_{0,j}$ . Each entry  $(\alpha, \beta)$  of the circulant matrix is defined as:

$$V_{0,j}(\alpha, \beta) = v_{0,j}[(\alpha - \beta) \bmod L] \quad (19)$$

where  $\alpha$  and  $\beta$  are the row and column indices, respectively, for  $\alpha, \beta \in \{0, 1, \dots, L-1\}$ .

To illustrate this relationship, consider a system with  $\mathbf{a}_0 = [4/1, 0, 50^\circ, 0, 35.7^\circ, 0]^T$  and uniformly spaced  $N = 2$  satellites. The corresponding seed satellite access profile observed from the target  $\mathcal{J} = \{(\phi = 36.7^\circ\text{N}, \lambda = 137.48^\circ\text{E})\}$  (a point) with  $\varepsilon_{min} = 10^\circ$  is shown in the top part of Fig. 6. The constellation pattern vector, shown in the middle part of the figure, has two unit impulses at  $n = 0$  and  $n = 359$  to represent temporal locations of two satellites with respect to the seed satellite. In this case, the first satellite of the system is essentially identical to the seed satellite (i.e., a unit impulse at  $n = 0$ ). The circular convolution between the seed satellite access profile and the constellation pattern vector yields the coverage timeline shown in the bottom part of the figure.

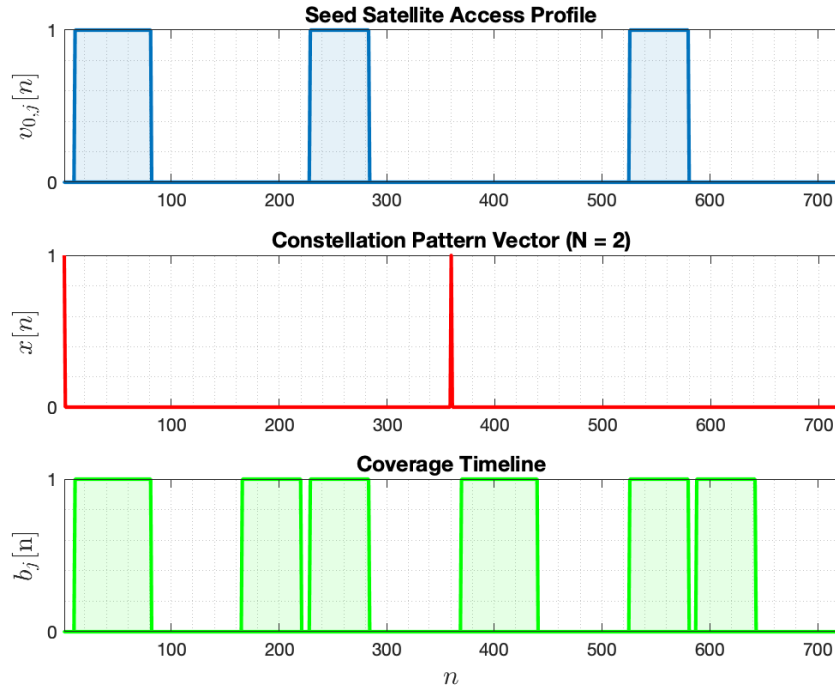


**Fig. 6** Circular convolution of seed satellite access profile and constellation pattern vector

This formulation exhibits a *common characteristics-distribution-performance* type of decomposition of the satellite constellation architecture. It is important to note that in the realm of physics, this circular convolution relationship is analogous to treating the access profile and the constellation pattern vector as discrete-time signals and the coverage timeline as the response of the system (see Appendix C). We shall hereafter refer to this type of satellite constellation design decomposition into three vectors  $v_{0,j}$ ,  $x$ , and  $b_j$  as the *APC decomposition*, following the acronyms of the seed satellite Access profile, constellation Pattern, and Coverage timeline. Methods that are derived based on the APC decompositions are called *APC-based methods*.

## V. Regional Coverage Constellation Design Methods

### A. Problem Statement

A process of satellite constellation design specifically pertaining to the APC decomposition involves the determination of two main parts: (1) common orbital characteristics and (2) constellation pattern. Here, the orbital characteristics determine the overall shape of the constellation whereas the constellation pattern dictates the spatio-temporal distribution of the actual system satellites. Mathematically, a satellite constellation architecture design  $d$ , following the APC decomposition introduced herein, can be expressed as:

$$\mathbf{d} = [\mathbf{e}_0, \mathbf{x}]^T \quad (20)$$

The objective of this paper is to solve for the constellation pattern vector  $\mathbf{x}$  such that all elements of  $\mathbf{b}_j = (v_{0,j} \otimes \mathbf{x})[n]$  are greater than a designated  $f[n]$ -fold coverage threshold. The number of satellites required  $N$  then can be deduced from Eq. (16). The optimization of the reference orbital characteristics—the seed satellite orbital elements vector  $\mathbf{e}_0$ —is not considered, but instead, we assume this to be given. This is because the seed satellite profile is often constrained by the launch or mission constraints and cannot be determined by constellation design optimization solely; inclusion of the seed satellite profile is part of the future work. Two APC-based methods are introduced herein on this regard: While-Loop method and Binary Integer Programming (BIP) method.

## B. Method 1: While-Loop Method

A while-loop based method assumes a uniform temporal spacing between satellites along the ground track. Given a length  $L$  of the constellation pattern vector, the uniform temporal spacing constant  $\delta \in \mathcal{Z}_{>0}$  between satellites is defined as:

$$\delta = \frac{L}{N} \quad (21)$$

The uniform temporal spacing  $\delta$  is a non-zero positive integer that guarantees a feasible integer-indexing of the discrete-time  $x[n]$  vector. (Note that we can choose  $L$  such that  $\delta$  is an integer.)

The While-Loop constellation in the constellation pattern vector form is:

$$x[n] = \begin{cases} 1 & \text{for } n = \{0, \delta, \dots, (N-1)\delta\} \\ 0 & \text{otherwise} \end{cases} \quad (22)$$

By definition, the constellation pattern vector is populated by letting the first satellite of the constellation system take the place of the hypothetical seed satellite. Hence, the seed satellite access profile is identical to the first satellite access profile of the system,  $v_{0,j} = v_{1,j}$ . Note that a user is allowed to arbitrarily set the temporal location of the first satellite; this paper assumes  $n = 0$  to be the temporal location of the seed satellite for the While-Loop method.

The algorithm is to perform a while-loop until all elements of  $b_j[n]$  are greater than or equal to the designated threshold  $f_j[n]$ . The while-loop increments  $N$  at each iteration and halts only when the coverage requirement is satisfied as shown in Algorithm 1. The method therefore outputs the minimum feasible  $N$  for a given target and coverage requirement.



---

**Algorithm 1** While-loop method to compute  $x$ ,  $N$ , and  $b_j$ 


---

```

1: procedure WHILELOOPMETHOD( $v_{0,j}, f_j$ )
2:    $N = 1$ 
3:   while True do
4:      $\delta = L/N$ 
5:     Generate  $x[n]$  based on  $\delta$  as outlined in Eq. (22)
6:     Compute  $b_j[n] = v_{0,j}[n] \otimes x[n]$  via Eq. (17)
7:     if  $c_j = 1$  as in Eq. (13) then
8:       Break while-loop
9:     else
10:       $N = N + 1$ 
11:    end if
12:  end while
13:  Return  $x$ ,  $N$ , and  $b_j$ 
14: end procedure

```

---

For an area of interest consisting of multiple target points, a user may replace the line 7 with “if  $C = 1$  via Eq. (14) then”. This guarantees a while-loop until all target points are satisfactorily covered.

An overview of the while-loop method is shown in Fig. 7.

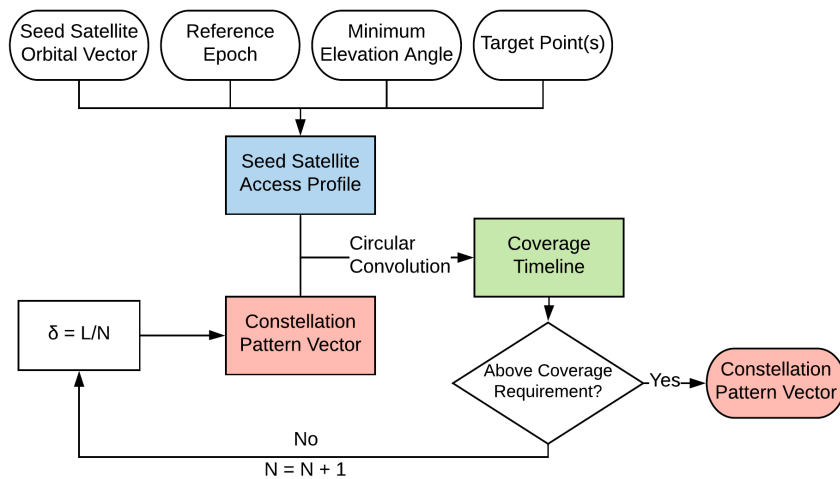


**Fig. 7 Overview of the While-Loop method**

### C. Method 2: Binary Integer Programming Method

Using the commutative property, a discrete-time circular convolution in Eq. (17) can be expressed in a linear form:

$$V_j \mathbf{x} = \mathbf{b}_j \quad (23)$$

where  $V_j \in \mathbb{Z}_2^{L \times L}$  is a circulant matrix that is fully specified by the seed satellite access profile  $v_{0,j}$  as shown in Eq. (24). The subscript 0 for the circulant matrix is dropped hereafter since we are only dealing with the circulant matrix of the seed satellite access profile.

$$V_j = \begin{bmatrix} v_{0,j}[0] & v_{0,j}[L-1] & v_{0,j}[L-2] & \cdots & v_{0,j}[1] \\ v_{0,j}[1] & v_{0,j}[0] & v_{0,j}[L-1] & \cdots & v_{0,j}[2] \\ & v_{0,j}[1] & v_{0,j}[0] & v_{0,j}[L-1] & \ddots & \vdots \\ \vdots & \vdots & & \ddots & \ddots & v_{0,j}[L-1] \\ v_{0,j}[L-1] & v_{0,j}[L-2] & \cdots & & v_{0,j}[1] & v_{0,j}[0] \end{bmatrix} \quad (24)$$

Each column of a circulant matrix  $V_j$  is identical to a circularly-shifted seed satellite access profile  $v_{0,j}$ . Eq. (23) can be shown in a matrix form,

$$\begin{bmatrix} v_{0,j}[0] & v_{0,j}[L-1] & v_{0,j}[L-2] & \cdots & v_{0,j}[1] \\ v_{0,j}[1] & v_{0,j}[0] & v_{0,j}[L-1] & \cdots & v_{0,j}[2] \\ \vdots & \vdots & \ddots & \ddots & \vdots \\ v_{0,j}[L-1] & v_{0,j}[L-2] & \cdots & v_{0,j}[1] & v_{0,j}[0] \end{bmatrix} \begin{bmatrix} x[0] \\ x[1] \\ \vdots \\ x[L-1] \end{bmatrix} = \begin{bmatrix} b_j[0] \\ b_j[1] \\ \vdots \\ b_j[L-1] \end{bmatrix} \quad (25)$$

An interesting observation is formalized. If we are given  $v_{0,j}$  and  $\mathbf{x}$ , then we can produce  $\mathbf{b}_j$ —this is the assumption of the While-Loop method at each iteration. Likewise, if we are given  $v_{0,j}$  and  $\mathbf{b}_j$ , then we can solve for  $\mathbf{x}$  via *deconvolution*, which one can solve Eq. (23) analytically in a closed-form,  $\mathbf{x} = V_j^{-1} \mathbf{b}_j$  ( $\det(V_j) \neq 0$ ), because the system is linear. Note that this vector  $\mathbf{b}_j$  represents the entire coverage timeline, and thus this analysis enables us to find a constellation pattern vector  $\mathbf{x}$  to satisfy a time-varying coverage demands  $\mathbf{f}_j$ .

However, the resulting  $\mathbf{x}$  may not necessarily be binary, which is a violation of the nature of the constellation pattern vector—a satellite cannot be represented in a decimal number. Therefore, in order to guarantee a physical quantification of satellites, we shall employ a binary integer programming to solve for  $\mathbf{x}$  that satisfies the inequality constraint:

$$V_j \mathbf{x} = \mathbf{b}_j \geq \mathbf{f}_j \quad (26)$$

Before we formalize the binary integer programming problem that solves Eq. (26), Sections V.C.1 and V.C.2 introduces linear properties associated with Eq. (23).

### 1. Multiple Target Points

Because the system is linear, we can extend this relationship to an area of interest that consists of *multiple target points*.

$$\begin{bmatrix} V_1 \\ V_2 \\ \vdots \\ V_{|\mathcal{J}|} \end{bmatrix} \mathbf{x} = \begin{bmatrix} \mathbf{b}_1 \\ \mathbf{b}_2 \\ \vdots \\ \mathbf{b}_{|\mathcal{J}|} \end{bmatrix} \quad (27)$$

where  $|\mathcal{J}|$  is the cardinality of a target point set  $\mathcal{J}$ . Eq. (27) has the dimension of  $(|\mathcal{J}|L \times L) \cdot (L \times 1) = (|\mathcal{J}|L \times 1)$ .

The augmented circulant matrix on the left-hand side is a matrix of matrices obtained by appending all circulant matrices  $V_1, \dots, V_{|\mathcal{J}|}$  linearly. Similarly, the augmented coverage timeline vector is also obtained by appending all coverage timeline vectors  $\mathbf{b}_1, \dots, \mathbf{b}_{|\mathcal{J}|}$  linearly. Here, the constellation pattern vector  $\mathbf{x}$  represents a single constellation configuration that satisfies the augmented linear condition.

### 2. Multiple Sub-Constellations

Another new direction of linearity is observed regarding having multiple sub-constellations. We consider a constellation system consisting of *multiple sub-constellations* with different seed satellite access profiles,  $\mathbf{v}_{0,j}^1, \dots, \mathbf{v}_{0,j}^z, \dots, \mathbf{v}_{0,j}^{|\mathcal{Z}|}$  where superscript  $z$  denotes an index of a sub-constellation,  $\mathcal{Z}$  is a set of sub-constellations, and  $|\mathcal{Z}|$  represents its cardinality. Each sub-constellation seed satellite access profile is computed based on its seed satellite orbital elements vector  $\mathbf{a}_0$  and the modified minimum elevation angle threshold  $\varepsilon_{j,min}^z[n]$ ,  $j \in \mathcal{J}$ ,  $z \in \mathcal{Z}$ ,  $n \in \{0, \dots, L-1\}$ , which is only applicable to the BIP method (since the While-Loop method cannot define multiple sub-constellations). The goal of the multiple sub-constellation system is to satisfy a common coverage requirement over a single target point  $j$ .

$$\begin{bmatrix} V_j^1 & V_j^2 & \dots & V_j^{|\mathcal{Z}|} \end{bmatrix} \begin{bmatrix} \mathbf{x}^1 \\ \mathbf{x}^2 \\ \vdots \\ \mathbf{x}^{|\mathcal{Z}|} \end{bmatrix} = \mathbf{b}_j \quad (28)$$

where the dimension of the system is  $(L' \times |\mathcal{Z}|L') \cdot (|\mathcal{Z}|L' \times 1) = (L' \times 1)$ . The matched dimension  $L'$  is explained in the following paragraph.

Each sub-constellation can have a different  $N_D$  value for  $\tau = N_P/N_D$ , therefore, the simulation periods  $N_D^1, \dots, N_D^{|\mathcal{Z}|}$  of respective 1,  $\dots$ ,  $|\mathcal{Z}|$ th sub-constellations must be *matched*, that is,  $N_D' = \text{lcm}(N_D^1, \dots, N_D^{|\mathcal{Z}|})$  where  $\text{lcm}(\cdot)$  is the least common multiple function. For example, consider a case of a system of two sub-constellations with  $N_D^1 = 1$  and  $N_D^2 = 2$  for  $z = 1$  and  $z = 2$ , respectively. An example of the lengths of vectors for  $N_D^1 = 1$  and  $N_D^2 = 2$  can be  $L = 719$  and

$L = 1438$ , respectively (i.e.,  $t_{step} \approx 120$  sec). The matched dimension, or a least common multiple between  $N_D^1$  and  $N_D^2$ , is  $N'_D = \text{lcm}(1, 2) = 2$ . Therefore, the matched length of vectors  $L'$  is equal to 1438. In order to match the length of the seed satellite access profile, one must augment each seed satellite access profile linearly as shown in Fig. 8. For this example case, one would need to linearly augment one additional  $\mathbf{v}_{0,j}^1$  to match the length of  $\mathbf{v}_{0,j}^2$ .

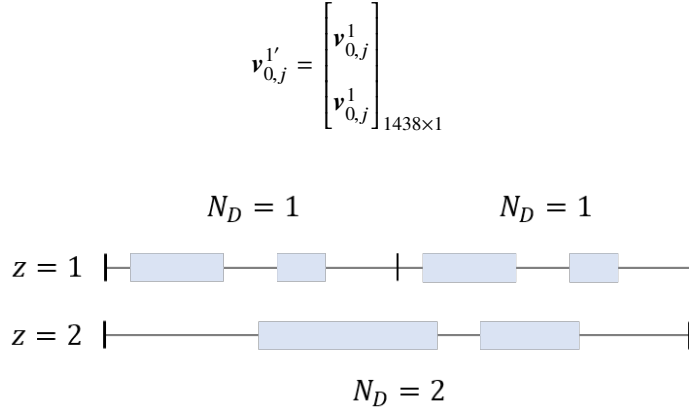


**Fig. 8 Matching of lengths of vectors for augmented operation**

### 3. A System of Multiple Sub-Constellations for Multiple Target Points

Combining both directions of linearity—multiple target points and multiple sub-constellations—we get the following generalized governing relationship:

$$\begin{bmatrix} V_1^1 & V_1^2 & \dots & V_1^{|\mathcal{Z}|} \\ V_2^1 & V_2^2 & \dots & V_2^{|\mathcal{Z}|} \\ \vdots & \vdots & \ddots & \vdots \\ V_{|\mathcal{J}|}^1 & V_{|\mathcal{J}|}^2 & \dots & V_{|\mathcal{J}|}^{|\mathcal{Z}|} \end{bmatrix}_{|\mathcal{J}|L' \times |\mathcal{Z}|L'} \begin{bmatrix} \mathbf{x}^1 \\ \mathbf{x}^2 \\ \vdots \\ \mathbf{x}^{|\mathcal{Z}|} \end{bmatrix}_{|\mathcal{Z}|L' \times 1} = \begin{bmatrix} \mathbf{b}_1 \\ \mathbf{b}_2 \\ \vdots \\ \mathbf{b}_{|\mathcal{J}|} \end{bmatrix}_{|\mathcal{J}|L' \times 1} \quad (29)$$

Which can be expressed in an indexed equation form:

$$\sum_{z=1}^{|\mathcal{Z}|} V_j^z \mathbf{x}^z = \mathbf{b}_j, \quad \forall j \in \mathcal{J} \quad (30)$$

where the subscript  $j$  is the target point index and the superscript  $z$  is the sub-constellation index.

The physical interpretation of Eq. (29) is as follows: it represents a system of multiple sub-constellations that simultaneously satisfies the coverage requirements imposed by multiple target points. Here, each multiple sub-constellation may exhibit its own unique orbital characteristics. For example, a sub-constellation ( $z = 1$ ) may be placed on a critically inclined elliptic orbit while a sub-constellation ( $z = 2$ ) may be placed on a circular low Earth orbit. Similarly, each target point may impose an independent coverage requirement. For example, a target point ( $j = 1$ ) may

require a continuous single fold coverage whereas a target point ( $j = 2$ ) may require a sinusoidal-like time-varying coverage fluctuating between the double and triple folds. It is the goal of the binary integer programming to determine the satellite constellation configurations  $\mathbf{x}^1, \dots, \mathbf{x}^z, \dots, \mathbf{x}^{|\mathcal{Z}|}$  that satisfies this complex relationship.

#### 4. Binary Integer Programming Problem Formulation

Let us assume that we want to achieve a  $f_j$ -fold coverage system ( $\forall j \in \mathcal{J}$ ) with given  $\mathbf{v}_{0,j}^1, \dots, \mathbf{v}_{0,j}^z, \dots, \mathbf{v}_{0,j}^{|\mathcal{Z}|}$  vectors. For cases in which we cannot solve for  $\mathbf{x}$  in a closed-form, we can employ a binary integer programming as shown in Eq. (31). Solving the most general form of the problem, Eq. (30), via BIP yields an optimal solution in the form of “a system of multiple sub-constellations that simultaneously satisfies the coverage requirements over multiple target points.”

$$\begin{aligned}
 & \underset{\mathbf{x}}{\text{minimize}} && \sum_{n=0}^{L-1} x[n] \\
 & \text{subject to} && \sum_{z=1}^{|\mathcal{Z}|} V_j^z x^z \geq f_j, \quad \forall j \in \mathcal{J} \\
 & && x[n] \in \{0, 1\} \quad \forall n = \{0, 1, \dots, L' - 1\}
 \end{aligned} \tag{31}$$

where the binary constraint is imposed on the elements of the constellation pattern vector  $\mathbf{x}$  to reflect the physical quantification of satellites.

Unlike the While-Loop method, the resulting constellation pattern vector of the BIP method does not necessarily make the first satellite of the system take the position of the seed satellite. Therefore, there are cases where the seed satellite remains hypothetical. This is illustrated in examples in Section VI.

An overview of the Binary Integer Programming method is shown in Fig. 9.

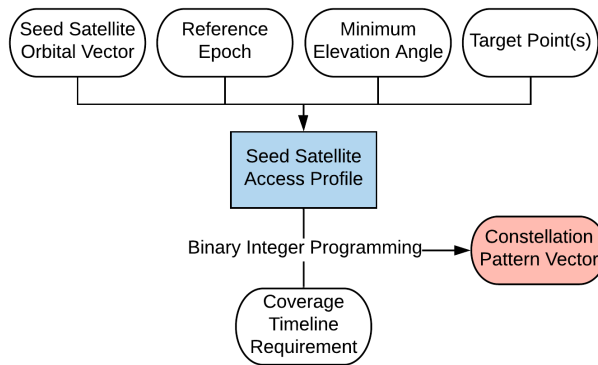


**Fig. 9 Overview of the Binary Integer Programming method**

#### D. Derivation of $\Omega$ and $M$ from the Constellation Pattern Vector

Once the aforementioned methods derive a constellation pattern vector, it must be post-processed to extract interpretable orbital information—a set of  $[\Omega, M]_k$  where  $k$  is the index of the satellite. This section introduces the

derivation of  $[\Omega, M]$  set from the constellation pattern vector.

In the discrete-time domain, there are  $L$  number of permissible  $[\Omega, M]$  sets that allow for a common ground track constellation. This is because the constellation pattern vector  $\mathbf{x}$  has the length of  $L$  and hence the maximum number of satellites it can define is equal to  $L$ . One can find  $[\Omega, M]$  sets by solving a system of equations:

$$N_P(\Omega_q - \Omega_0) + N_D(M_q - M_0) = 0 \text{ mod } (2\pi) \quad (32a)$$

$$\Omega_q = q \frac{2\pi N_D}{L} + \Omega_0 \quad (32b)$$

where  $q$  is the generalized index for Eq. (33). Note that Eq. (32a) is rearranged from Eq. (6) [30].

To find all permissible sets in the  $[\Omega, M]$ -space, one would need to explore all discrete-time instants of  $n$ . However, for either While-Loop or BIP methods, one would only need to explore  $n_k$  discrete-time instants where only satellites exist. Solving Eq. (32) then yields  $M_q$ .

Fig. 10 illustrates a complete and comprehensive analysis of the  $[\Omega, M]$ -space of Example 1 in Section VI. For  $N_D = 1$ , the total number of sampling points or lengths of vectors (e.g.,  $\mathbf{v}, \mathbf{b}, \mathbf{x}$ ) is  $L = 719$  (i.e.,  $t_{step} \approx 120$  sec). Therefore, there are  $L = 719$  number of *permissible* sets of  $[\Omega, M]$  which a satellite can be placed. Analyzing the patterns in Fig. 10, the While-Loop set depicts a lattice-like symmetry in the  $[\Omega, M]$ -space whereas the BIP set exhibits an asymmetry in the  $[\Omega, M]$ -space.

$$\text{To find permissible sets: } q \triangleq n \in \{0, \dots, L - 1\} \quad (33a)$$

$$\text{To find While-Loop or BIP sets: } q \triangleq n_k \quad (33b)$$

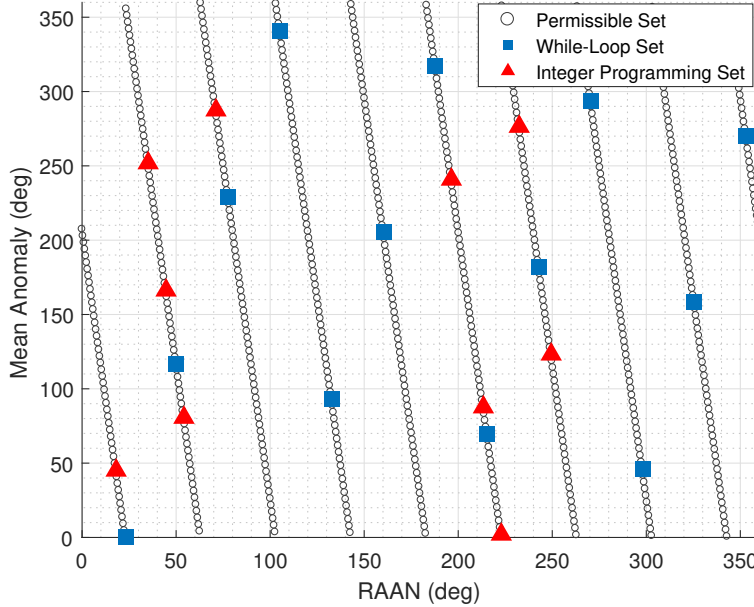


**Fig. 10** Illustration of permissible set, While-Loop set, and Binary Integer Programming set in the  $[\Omega, M]$ -space of Example 1, Section VI

## VI. Illustrative Examples

This section aims to demonstrate the general applicability of and the computational efficiency associated with the proposed methods under various mission profiles. Seven illustrative examples are uniquely set up by varying orbital characteristics, area of interest properties, minimum elevation angle, and coverage requirement.

All illustrative examples are conducted on a Intel Core i7-4790 Processor @3.60 GHz platform. For integer programming problems, a Mixed-Integer Programming model by Gurobi 8.0.1 is used; the original termination setting is used except for the time-limit of 10 000 sec [36].

All examples are referenced to the epoch 15 Feb 2017 12:00:00.000. The lengths of vectors are set to  $L = 719$  for  $N_D = 1$  and  $L = 1438$  for  $N_D = 2$ , which correspond to a uniform sampling of an elevation angle function at the time step of approximately  $t_{step} \approx 120$  sec. The referenced ellipsoid model is the World Geodetic System 1984 (WGS 84). A ground station or a user terminal is assumed to be placed on a target point and no consideration of inter-satellite link communications is assumed. No slewing capability of satellites is assumed (all satellites point to their nadir direction). Lastly, we assume the utilization of satellite maneuvers to correct and maintain identical ground track throughout the satellite lifetime, negating the perturbation effects other than the  $J_2$  effect.

For the sake of simple demonstration purposes only, this paper further assumes the minimum elevation angle threshold definition such that the minimum elevation angle threshold  $\varepsilon_{j,min}[n]$  imposed on a target point  $j$  at discrete-time instant  $n$  is identical to a constant value  $\varepsilon_{min}$  for all  $j \in \mathcal{J}$  and for all  $n \in \{0, \dots, L - 1\}$ . Note that one can still impose

the minimum elevation angle threshold definition as it is as shown in Eq. (10) for all cases demonstrated in this paper. Also, note that this paper does not use the definition  $\varepsilon_{j,min}^z[n]$  from Section V.C due to the multiple sub-constellation definition inapplicability to the While-Loop method. Therefore, modifying Eq. (10),

$$\varepsilon_{j,min}[n] = \varepsilon_{min}, \quad \forall j \in \mathcal{J}, \quad \forall n \in \{0, \dots, L - 1\}$$

Table 1 is a list of variables used for each example study. Note that the seed satellite orbital elements vector  $\mathbf{a}_0$  takes the form of  $[\tau, e, i, \omega, \Omega_0, M_0]^T$ . The first four illustrative examples focus on varying orbital characteristics, minimum elevation angle, and coverage requirement over a single target point. Examples 5 and 6 aim to demonstrate the general applicability of proposed methods considering an area of interest composed of multiple target points. Lastly, Example 7 aims to illustrate the most general case possible considering a system with multiple sub-constellations for multiple target points. All illustrative example results are summarized in Table 2. The rest of the section introduces the details of each illustrative case.

**Table 1 Example Setup**

Example	$\mathbf{a}_0^T$	$\varepsilon_{min}$	$\mathcal{J}$	$f$
1	[9/1, 0, 40°, 0, 23.1°, 0]	10°	{( $\phi = 36.7^\circ\text{N}, \lambda = 137.48^\circ\text{E}$ )}	<b>1</b>
2	[5/2, 0, 20°, 0, 90°, 0]	20°	{( $\phi = 36.7^\circ\text{N}, \lambda = 137.48^\circ\text{E}$ )}	<b>2</b>
3	[7/1, 0, 50°, 0, 25.9°, 0]	10°	{( $\phi = 36.7^\circ\text{N}, \lambda = 137.48^\circ\text{E}$ )}	Square Wave
4	[12/1, 0, 102.89°, 0, 325.4°, 0]	5°	{( $\phi = 19.4^\circ\text{N}, \lambda = 155.28^\circ\text{W}$ )}	
5	[5/1, 0, 30°, 0, 135.97°, 0]	10°	{CONUS} (41 Target Points)	<b>1</b>
6	[8/1, 0.075, 63.435°, 270°, 0, 0]	20°	{(NYC, USA), (London, UK), (Seoul, South Korea)}	<b>1</b>
7	$\mathbf{a}_0^{1T} = [8/1, 0, 70^\circ, 0, 0, 0]$	10°	{( $\phi = 64.14^\circ\text{N}, \lambda = 21.94^\circ\text{W}$ ),	<b>1</b>
	$\mathbf{a}_0^{2T} = [6/1, 0, 40^\circ, 0, 0, 0]$		( $\phi = 19.07^\circ\text{N}, \lambda = 72.87^\circ\text{E}$ )}	

**Table 2 Example Results**

Example	While-Loop		Binary Integer Programming	
	$N$	Time Cost (sec)	$N$	Time Cost (sec)
1	13	0.01	10	12.02
2	13	0.01	13	65.99
3	14	0.01	12	800.69
4	33	0.15	20	10000
5	10	0.03	9	101.15
6	19	0.01	12	3187.93
7	-	-	9 (1st: 4, 2nd: 5)	4190.45



### A. Example 1. Medium Earth Orbit

A point target is located at Japan,  $\mathcal{J} = \{(\phi = 36.7^\circ\text{N}, \lambda = 137.48^\circ\text{E})\}$ , with  $\varepsilon_{min} = 10^\circ$ . A seed satellite orbital element vector  $\mathbf{a}_0 = [9/1, 0, 50^\circ, 0, 23.1^\circ, 0]^T$  is assumed (an altitude of 3343.5 km). The objective is to achieve the single continuous coverage ( $f[n] = \mathbf{1}$ ).

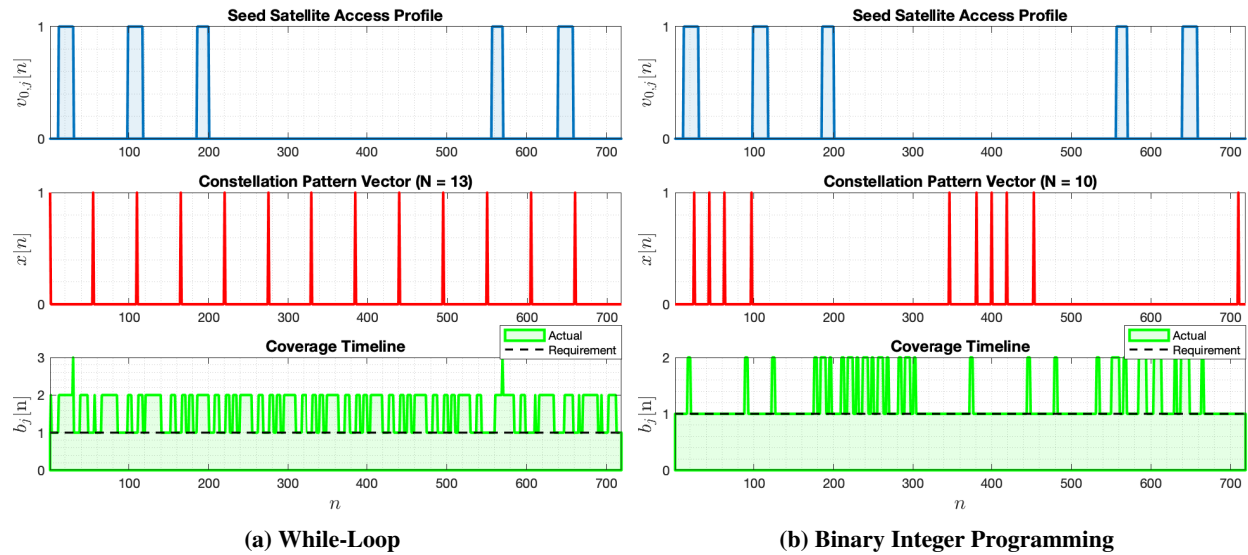


Fig. 11 Example 1. Generation of satellite constellations

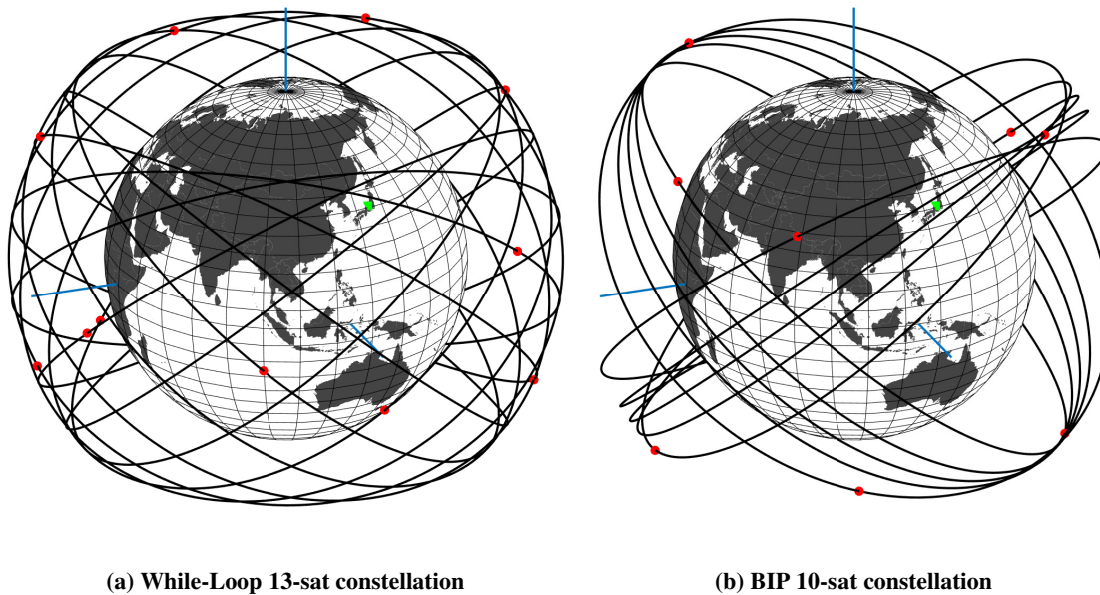
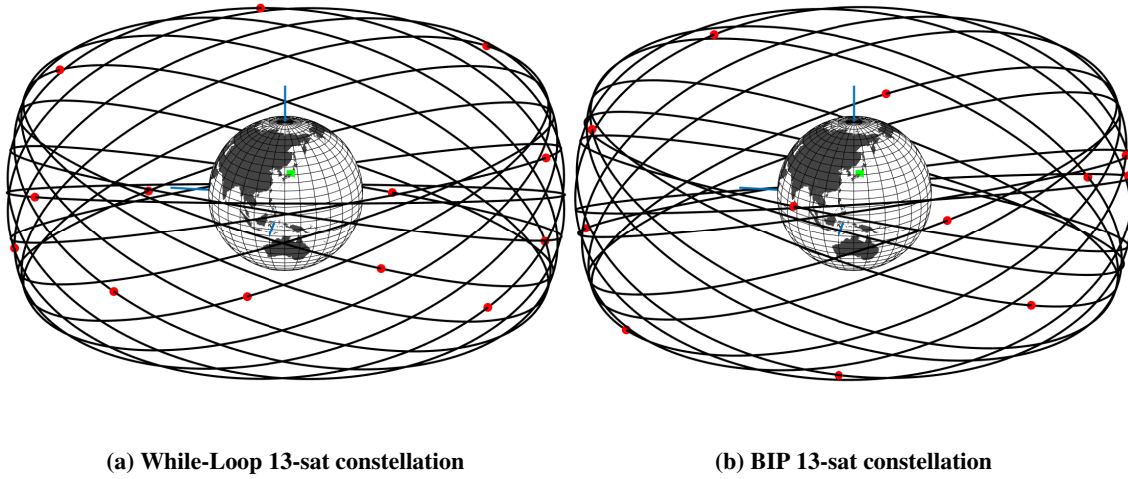


Fig. 12 Example 1. 3-D view of generated constellations (the ECI reference frame is represented in right-handed basis)

The While-Loop method yields 13 satellites while the BIP method yields 10 satellites. The results indicate that the BIP method found the optimal constellation pattern vector by breaking the symmetry. Comparing the time cost, the





**Fig. 14 Example 2. 3-D view of generated constellations**

### C. Example 3. Square Wave Function Coverage

A point target is located at Japan,  $\mathcal{J} = \{(\phi = 36.7^\circ\text{N}, \lambda = 137.48^\circ\text{E})\}$ , with  $\varepsilon_{min} = 10^\circ$ . A seed satellite orbital element vector  $\mathbf{a}_0 = [7/1, 0, 50^\circ, 0, 25.9^\circ, 0]^T$  is assumed (an altitude of 5239.5 km). The objective is to achieve a specialized threshold function, specifically, a square wave function ( $f[n] = [2, 2, 2, \dots, 1, 1, \dots, 1, \dots, 2, 2, 2]^T$ ).

A coverage requirement is now time-dependent; the square wave function is assumed between values 1 and 2. This requires that some part of the day must be continuously covered by at least two satellites and by at least one satellite during another part of the day. This type of example can be extended to a case with a temporal demand distribution. For example, a communication satellite constellation may require two satellites during the day for doubled-capacity and one satellite during the night for a quiescent mode.

As shown in Fig. 15, the BIP constellation produces a coverage timeline that closely follows the temporally-varying coverage requirement. Such a coverage timeline is possible since the integer programming aims to minimize the discrepancy between the coverage timeline and the coverage requirement. This is not the case for the While-Loop method due to its symmetrical coverage timeline, which aims to fulfill the maximum coverage requirement point (two in this case), thereby preventing itself from filling the coverage discrepancy between the timeline and the requirement.

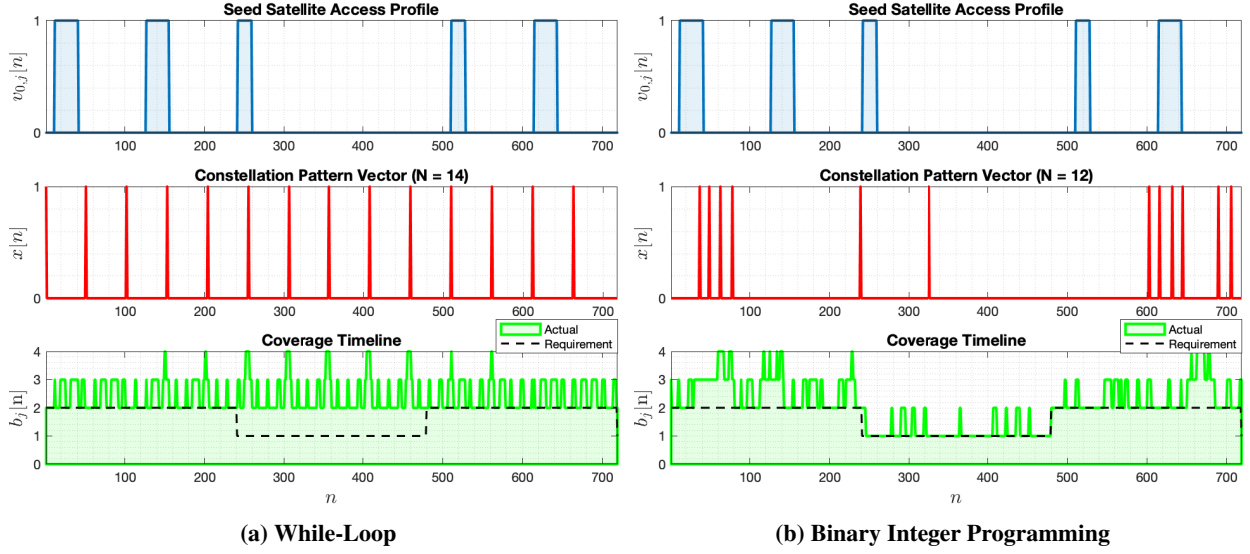


Fig. 15 Example 3. Generation of satellite constellations

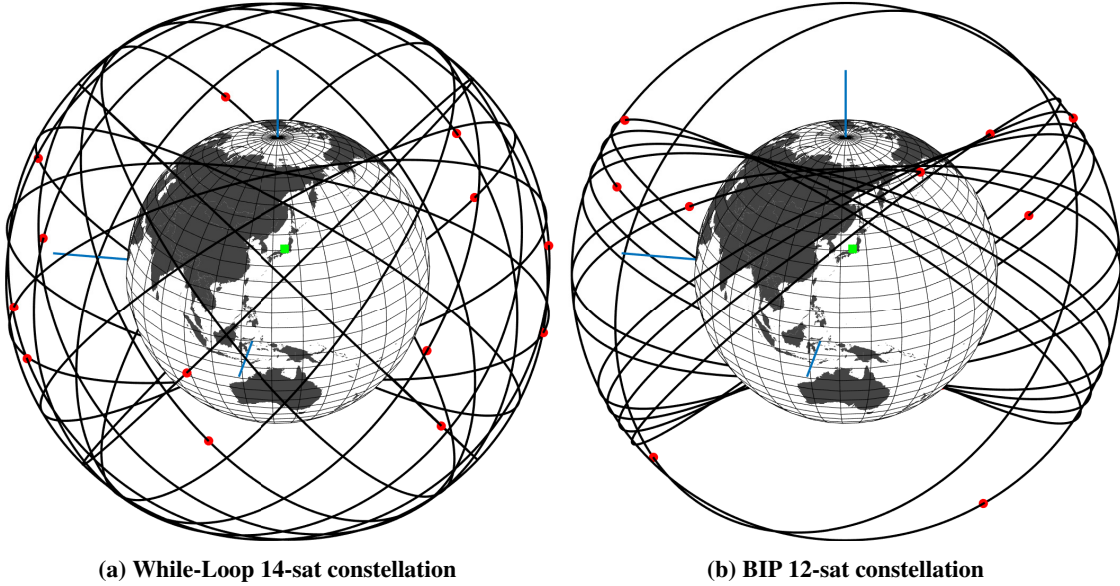


Fig. 16 Example 3. 3-D view of generated constellations

#### D. Example 4. Repeating Sun Synchronous at Low Earth Orbit

This example depicts a mission in which a constellation must continuously monitor a volcano eruption at a target point Kīlauea, Hawaii. A point target located at  $\mathcal{J} = \{(\phi = 19.4^\circ\text{N}, \lambda = 155.28^\circ\text{W})\}$  and requires  $\varepsilon_{min} = 5^\circ$ . The local time of the ascending node is set to 12:00:00.000. A seed satellite orbital element vector  $\alpha_0 = [12/1, 0, 102.89^\circ, 0, 325.4^\circ, 0]^T$  is assumed (an altitude of 1676.5 km). The objective is to achieve the single continuous coverage ( $f[n] = 1$ ).

Low earth orbit constellation systems generally require a greater number of satellites than their higher orbit counterparts. This illustrative example suggests that compared with the symmetrical While-Loop method, the BIP

method can greatly reduce the total number of satellites required in the system for low earth orbit cases—33-satellite-While-Loop-system vs. 20-satellite-BIP-system.

The optimization time limit is triggered for the BIP case. The resulting constellation configuration by the BIP method may not be a global optimal solution.

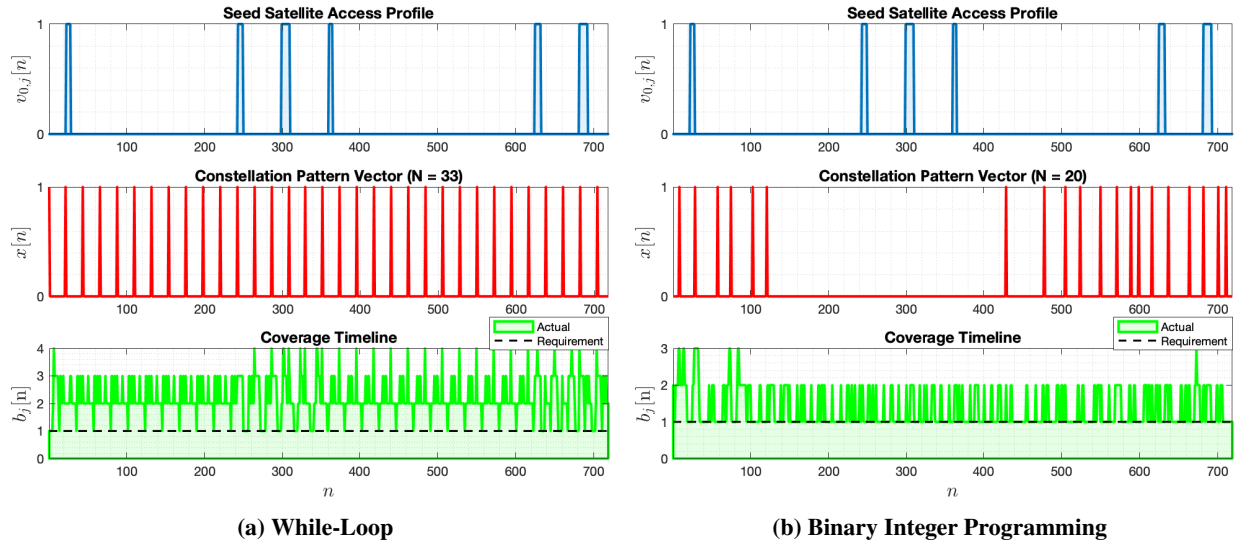


Fig. 17 Example 4. Generation of satellite constellations

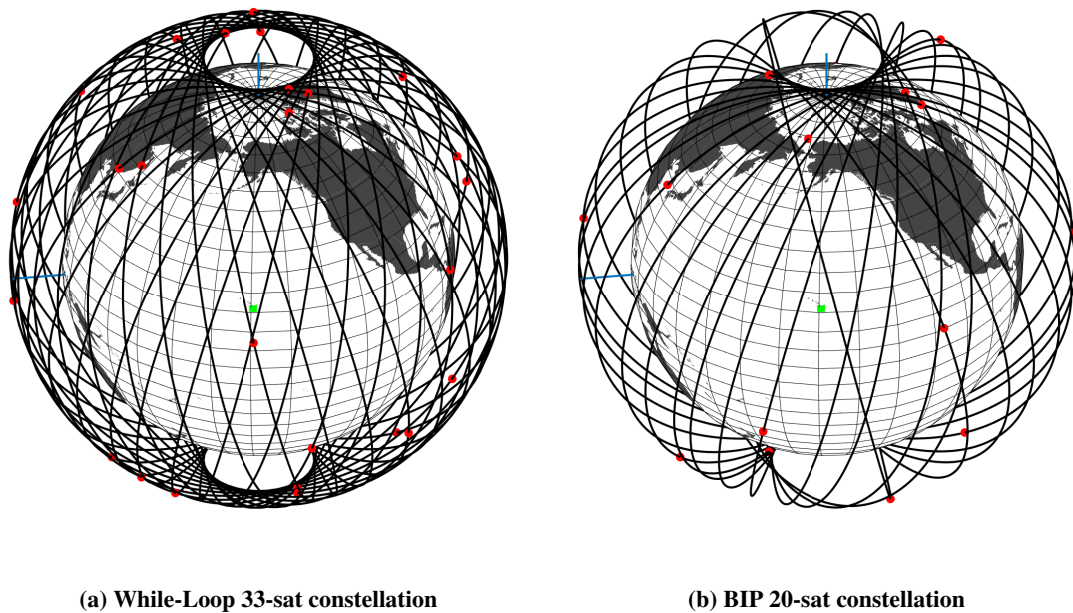


Fig. 18 Example 4. 3-D view of generated constellations

### E. Example 5. Area Target (CONUS)

For this example, we consider the contiguous United States (CONUS) as the area of interest. The CONUS is gridded out with a total of 41 target points in a 4°-by-4° resolution (longitude-by-latitude) as shown in Fig. 19. All target points require  $\varepsilon_{min} = 10^\circ$ . A seed satellite orbital element vector  $\mathbf{oe}_0 = [5/1, 0, 30^\circ, 0, 135.97^\circ, 0]^T$  is assumed (an altitude of 8034.6 km). The objective is to achieve the single continuous coverage ( $f[n] = \mathbf{1}$ ) over all target points.

This example illustrates the linear property of the circulant matrix form as in Eq. (27).

$$\begin{bmatrix} V_1 \\ V_2 \\ \vdots \\ V_{41} \end{bmatrix} \mathbf{x} = \begin{bmatrix} \mathbf{b}_1 \\ \mathbf{b}_2 \\ \vdots \\ \mathbf{b}_{41} \end{bmatrix}$$

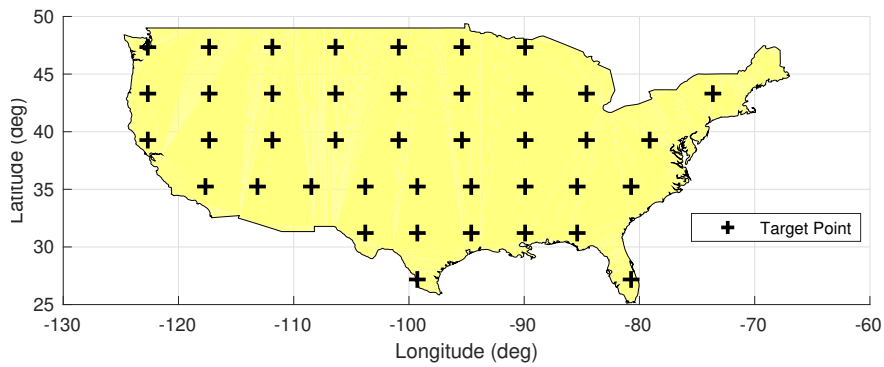


**Fig. 19** Example 5. Contiguous United States and its gridded target points (4°-by-4° resolution)



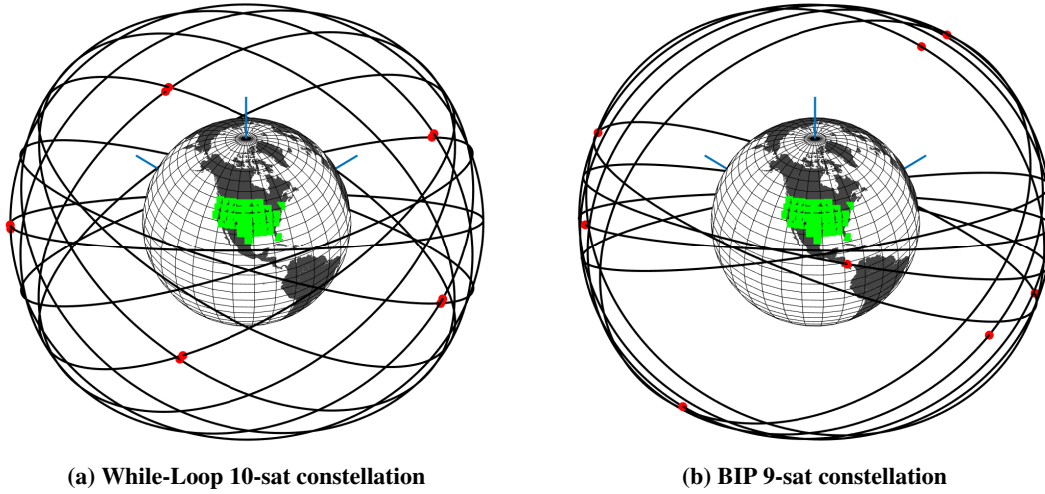


**Fig. 20 Example 5. 3-D view of generated constellations**

**F. Example 6. Discontiguous Multiple Targets and Critically Inclined Elliptic Orbit**

For this example, we consider targets that are discontiguous to each other. Three target points are positioned on New York City, USA, London, UK, and Seoul, South Korea:  $\mathcal{J} = \{(\phi = 40.71^\circ\text{N}, \lambda = 74.00^\circ\text{W}), (\phi = 51.50^\circ\text{N}, \lambda = 0.12^\circ\text{W}), (\phi = 37.56^\circ\text{N}, \lambda = 126.97^\circ\text{E})\}$ . The target points are shown in Fig. 21. All target points require  $\varepsilon_{min} = 20^\circ$ . A seed satellite orbital element vector  $\mathbf{a}_0 = [8/1, 0.075, 63.435^\circ, 270^\circ, 0, 0]^T$  is assumed (critically inclined elliptical orbit with the apogee over the northern hemisphere). The objective is to achieve the single continuous coverage ( $f[n] = \mathbf{1}$ ) over all target points.

The resulting constellations shown in Fig. 22 fulfill the single continuous coverage requirement over all target points that are discontiguous to each other.

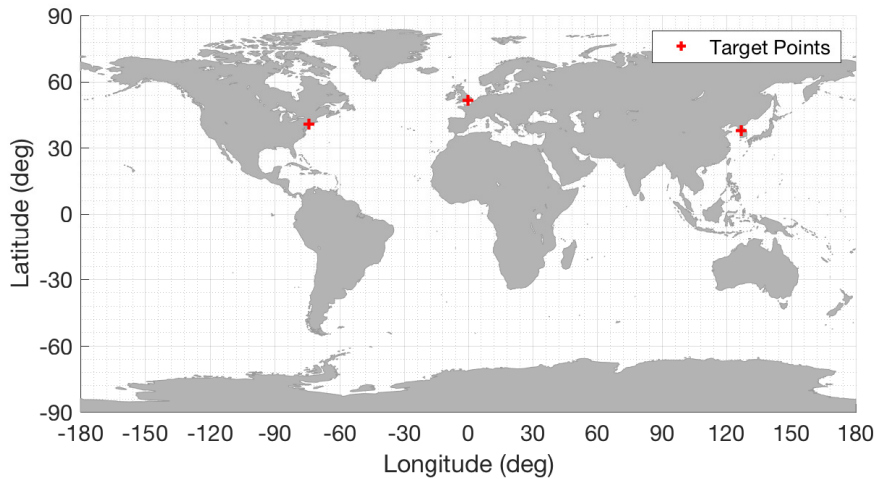
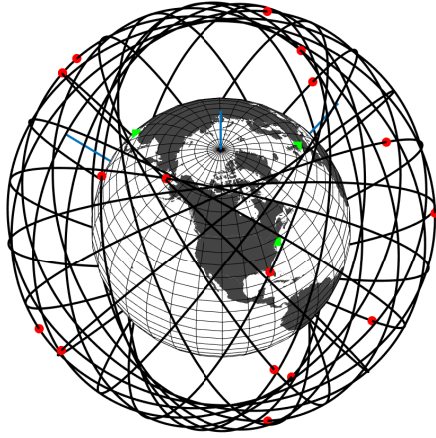
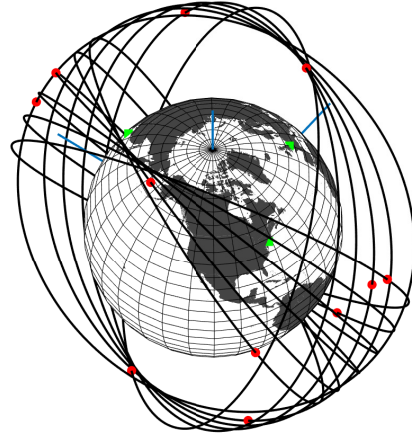


**Fig. 21 Example 6. Target points—NYC, London, Seoul**



(a) While-Loop 19-sat constellation



(b) BIP 12-sat constellation

Fig. 22 Example 6. 3-D view of generated constellations

### G. Example 7. A System of Multiple Sub-Constellations over Multiple Target Points

We consider the most general case the BIP method can provide: a system of multiple sub-constellations over multiple target points. In this example, two target points are considered in the target set  $\mathcal{J} = \{(\phi = 64.14^\circ\text{N}, \lambda = 21.94^\circ\text{W}), (\phi = 19.07^\circ\text{N}, \lambda = 72.87^\circ\text{E})\}$ : Reykjavík, Iceland ( $j = 1$ ) and Mumbai, India ( $j = 2$ ). All target points require  $\varepsilon_{min} = 10^\circ$ . The objective is to achieve the single continuous coverage ( $f[n] = \mathbf{1}$ ) over all target points.

Two sub-constellations are considered:  $\mathbf{x}_0^1 = [8/1, 0, 70^\circ, 0, 0, 0]^T$  (an altitude of 4149.2 km) and  $\mathbf{x}_0^2 = [6/1, 0, 40^\circ, 0, 0, 0]^T$  (an altitude of 6380.2 km). The goal of the BIP method is to optimize both  $\mathbf{x}^1$  and  $\mathbf{x}^2$  sub-constellations concurrently that satisfy the augmented linear condition:

$$\begin{bmatrix} V_1^1 & V_1^2 \\ V_2^1 & V_2^2 \end{bmatrix} \begin{bmatrix} \mathbf{x}^1 \\ \mathbf{x}^2 \end{bmatrix} \geq \begin{bmatrix} f_1 \\ f_2 \end{bmatrix} \Leftrightarrow \{V_1^1 \mathbf{x}^1 + V_1^2 \mathbf{x}^2 \geq f_1, V_2^1 \mathbf{x}^1 + V_2^2 \mathbf{x}^2 \geq f_2\}$$



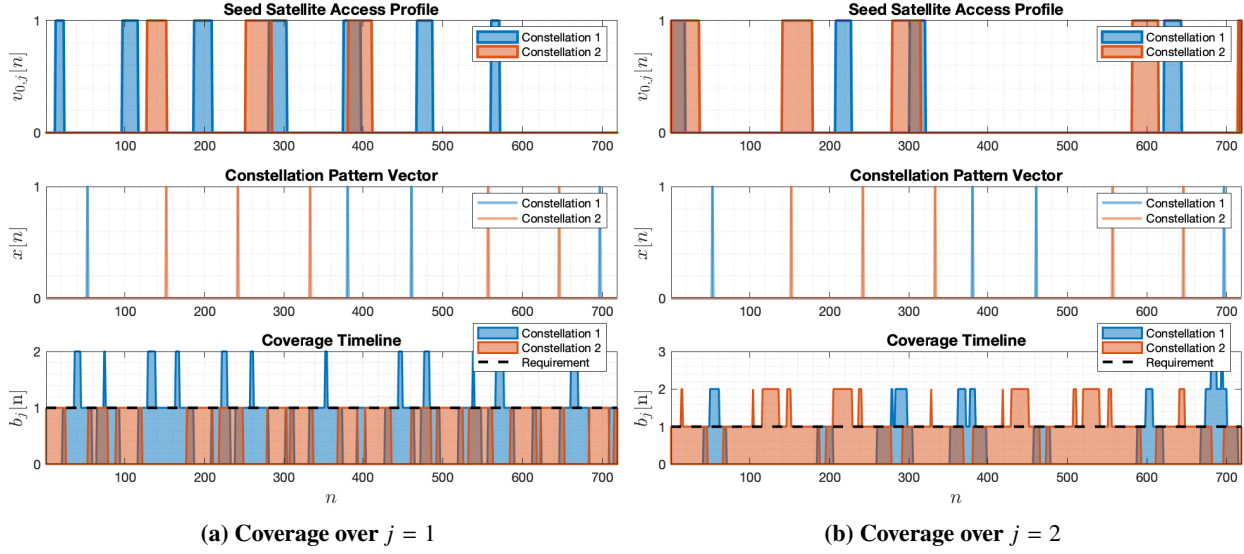


**Fig. 23 Example 7. Generation of satellite constellations**

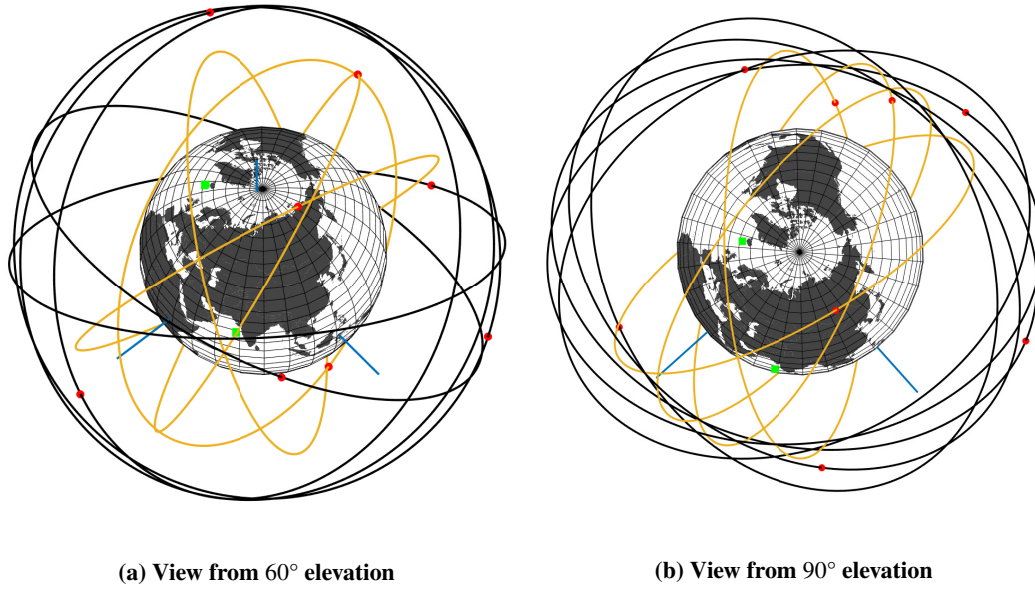


**Fig. 24 Example 7. 3-D view of BIP 9-sat constellation system**

Fig. 23 illustrates the benefit of the BIP method. Individually,  $z = 1$  sub-constellation provides 62.3% and 33.5% coverage over  $j = 1$  and  $j = 2$ , respectively and  $z = 2$  sub-constellation provides 61.2% and 86.6% coverage over  $j = 1$  and  $j = 2$ , respectively. No individual sub-constellation alone provides a full coverage over any target point. The BIP method concurrently optimizes  $\mathbf{x}^1$  and  $\mathbf{x}^2$  such that the continuous coverage over the whole target set  $\mathcal{J}$  is achieved while minimizing the total number of satellites from two sub-constellations. Note that in Fig. 23,  $\mathbf{x}^1$  and  $\mathbf{x}^2$  are identical in both sub-figures.

The optimized two-sub-constellation systems are shown in Fig. 24. The sub-constellation ( $z = 1$ ) colored in yellow

(lower altitude) is composed of four satellites while the sub-constellation ( $z = 2$ ) colored in black (higher altitude) is composed of five satellites for a total of nine satellites.

## H. Summary

This paper explored seven different cases to identify the general applicability of and the computational efficiency associated with the methods. A variety of orbits—circular vs. elliptic (critically inclined), prograde vs. retrograde, and low vs. high altitudes—and a variety of areas of interests—a single target point vs. multiple target points and contiguous vs. discontinuous—are considered. For all cases, the While-Loop method proved to be computationally efficient while the Binary Integer Programming method yielded the optimal solution. Both of these methods are generally applicable to any combination of orbit (must be critically inclined if elliptic, due to the  $J_2$  perturbation assumption) and area of interest. The BIP method has added benefit in that it can also simultaneously design multiple sub-constellations over a set of target point(s). A summary of two methods is shown in Table 3.

**Table 3 Summary of Two Methods**

Remarks	While-Loop	Binary Integer Programming
Given	$\nu_{0,j}, f_j$	$\nu_{0,j}, f_j$
Solve for	$\mathbf{x}$	$\mathbf{x}$
Multiple Target Points	Yes	Yes
Multiple Sub-Constellations	No	Yes
Resulting Constellation Type	Symmetric	Symmetric/Asymmetric
Computational Efficiency	Fast	Slow (depends on $L$ )

## I. Discussion of Limitations

There are some issues arising from the nature of the discretization. The discrete-time access profile is constructed via sampling a continuous-time elevation angle function of a satellite at every time-step  $t_{step}$ . Therefore, the results output by the proposed While-Loop and Binary Integer Programming methods may vary depending on the value of  $t_{step}$  due to coverage discrepancies in the continuous-time and discrete-time simulations. Also, the computation time to solve proposed methods largely depends on the level of discretization especially for the BIP method as the problem is NP-hard. The trade-off is: the smaller the value of  $t_{step}$ , the higher the fidelity of the simulation but the longer the time to solve for each method due to the longer lengths of access profile, constellation pattern vector, and coverage timeline.

The proposed method only computes an access profile for given  $N_D$  day(s) because of its assumed repeatability in the ground track. Because the orbital perturbation is only considered up to  $J_2$ , the access profile repeatability may not be consistent with actual coverage performance under various perturbations such as  $J_4$  higher-order terms, solar radiations,

atmospheric drag, or third body. All illustrative examples described herein assumed the utilization of satellite maneuvers to correct and maintain identical ground track throughout the satellite lifetime, negating the additional perturbation effects other than the  $J_2$  effect.

## VII. Conclusion

A semi-analytical approach to optimally design regional coverage satellite constellations is proposed. By treating the seed satellite access profile and the constellation pattern vector as discrete-time signals, a circular convolution between them creates the coverage timeline. We refer to this formulation as the APC decomposition of the satellite constellation system. Two methods are introduced: While-Loop and Binary Integer Programming. Both While-Loop and BIP methods take the same set of inputs—a seed satellite access profile and a coverage requirement—and outputs the minimum number of satellites required to satisfy the coverage requirement. The While-Loop method additionally enforces symmetry in the constellation pattern (i.e., a uniform distribution of satellites along the common ground track of the constellation system) and solves for the minimum number of satellites required in the system by incrementally increasing  $N$  until the coverage requirement is satisfied. On the contrary, the BIP method solves for constellation pattern vector  $\mathbf{x}$  where  $N$  and their temporal locations can be deduced by solving an integer programming problem. An analysis shows that the While-Loop method is fast and computationally efficient while the BIP method outputs optimal satellite constellation designs.

The circular convolution formulation allows linearity in both the multiple target points direction and multiple sub-constellations direction by matrix augmentation. A user can design (1) a single satellite constellation system that simultaneously satisfies the time-varying coverage requirement of an area target composed of multiple target points, (2) a system of multiple sub-constellations that satisfies the time-varying coverage requirement of a single target point, or (3) a combination of both, which is illustrated in Example 7. This formulation is especially useful for missions with complex satellite coverage requirements by representing it in a non-negative integer form—intermittent coverage or sinusoidal square wave-like coverage with temporal variations in satellite visibility demand (e.g., increased capacity during the day and reduced capacity during the night). Moreover, traditional figures of merit such as maximum revisit time can be easily implemented as a part of  $f[n]$ . Example 3 demonstrates the value of such time-dependent coverage requirement.

The methods proposed in this paper can be used as constellation design modules in larger optimization settings. By defining a set of seed satellite orbital elements as design variables  $[\tau, e, i, \omega, \Omega_0, M_0]^T$ , one can easily set up an optimization problem to design an optimal constellation (both orbital elements and constellation pattern as in Eq. (20)) for one or more target points. For a rapid preliminary analysis of the design space, the authors suggest the use of the While-Loop method. A further refinement can be accomplished by employing the BIP method with the obtained seed satellite orbital elements if at all the true optimal solution for the region of interest is desired.

## Appendix A. Expanded Ground Track View

The *expanded ground track view* spatially expands a ground track of a satellite and visualizes its ground track relative to the area of interest throughout the simulation period  $N_D$ . The area of interest and its mirrored images are positioned throughout the plot (the cyan squares in Figure 25) to provide temporal references. The expanded ground track view is especially useful when visualizing and correlating the access profile and the actual satellite ground track.

The following properties of the expanded ground track view are formalized for the repeating ground track with the period ratio of  $\tau = N_P/N_D$ .

- 1) The expanded ground track view is an extension of  $(N_P - 1)$  ordinary ground track views along the longitudinal direction. For example, as shown in Figure 25, the expanded view is an extension of three  $(N_P = 4)$  ordinary ground track views; the three vertical dashed lines indicate their boundaries.
- 2) Extending Property 1, the mirrored images of the area of interest are separated by  $2\pi$ .
- 3) The longitudinal displacement of the expanded ground track is  $2\pi(N_P - 1)$ .

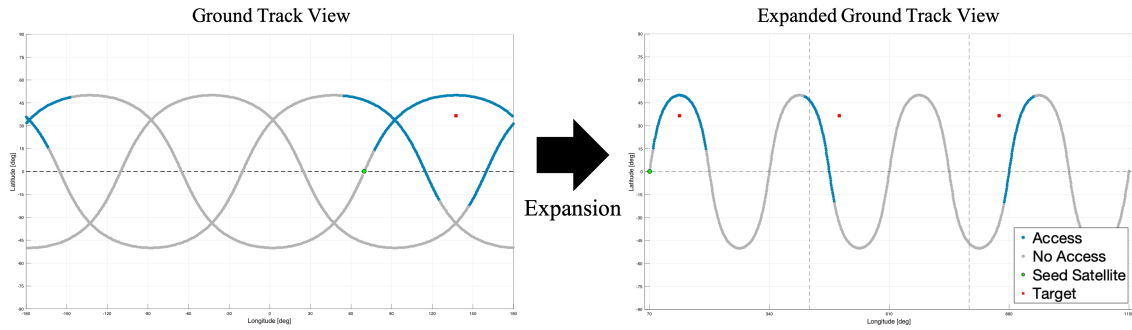


**Fig. 25** Full expansion of a ground track of  $\alpha_0 = [4/1, 0, 50^\circ, 0, 35.4^\circ, 0]$  referenced to the epoch 15 Feb 2017 12:00:00.000

## Appendix B. Derivation of Circular Convolution

To prove the circular convolution phenomenon, show that Eq. (12) is identical to Eq. (17). Begin by expanding Eq. (12), which is the summation of all access profiles:

$$b_j[n] = v_{1,j}[n] + v_{2,j}[n] + \cdots + v_{N,j}[n] \quad (34)$$

Each term of Eq. (34) can be represented as a multiple of  $v_{0,j}[n]$  and permutation matrix  $P_\pi^{n_k}$  due to the cyclic property of the assumed formulation. Recalling the definition from Eq. (11):

$$v_{k,j}[n] = P_\pi^{n_k} v_{0,j}[n]$$

where  $P_\pi$  is a permutation matrix with the dimension  $(L \times L)$  shown in Eq. (35). Note that  $I = P_\pi^0 = P_\pi^L$ .

$$P_\pi = \begin{bmatrix} 0 & 0 & 0 & \cdots & 1 \\ 1 & 0 & 0 & \cdots & 0 \\ 0 & 1 & 0 & \ddots & \vdots \\ \vdots & \vdots & & \ddots & \ddots \\ 0 & 0 & \cdots & 1 & 0 \end{bmatrix} \quad (35)$$

Substituting Eq. (11) into Eq. (34), we get the following equation:

$$b_j[n] = (P_\pi^{n_1} + P_\pi^{n_2} + \cdots + P_\pi^{n_N})v_{0,j}[n] \quad (36)$$

Eq. (36) is a superposition of cyclically shifted access profiles referenced to a seed satellite access profile. Here,  $n_k$  denotes the index of the relative time shift of the  $k$ th access profile with respect to the seed satellite access profile. Instead of only indicating the indices where only access profiles exist, one can generalize this to all time step  $n = \{0, \dots, L - 1\}$  following the definition of the constellation pattern vector in Eq. (15). Hence, Eq. (36) can be further deduced as:

$$b_j[n] = \left( x[0]P_\pi^0 + x[1]P_\pi^1 + \cdots + x[L-1]P_\pi^{L-1} \right) v_{0,j}[n] \quad (37)$$

The terms within the parenthesis in Eq. (37) is identical to the alternative analytical definition of the circulant matrix:

$$X \triangleq x[0]I + x[1]P_\pi^1 + \cdots + x[L-1]P_\pi^{L-1} \quad (38)$$

Finally, substituting Eq. (38) into Eq. (37), we can get:

$$\mathbf{b}_j = X\mathbf{v}_{0,j} \quad (39)$$

Using the commutative property of the circular convolution operator, Eq. (39) is identical to:

$$\mathbf{b}_j = V_{0,j}\mathbf{x} \quad (40)$$

This is identical to the definition of the circular convolution in Eq. (18) (which is Eq. (17)), thereby proving the circular convolutional nature of the formulation under the aforementioned assumptions.

## Appendix C. Circular Convolution in Frequency-Domain

Circular convolution is widely used in the realm of Fourier analysis. A circular convolution of two discrete-time signals in the time domain is equivalent to a multiplication of the corresponding discrete Fourier transforms (DFT) in the frequency domain:

$$b_j[n] = \sum_{m=0}^{L-1} v_{0,j}[m]x[(n-m) \bmod L] \leftrightarrow \mathcal{B}_j[k] = \mathcal{V}_{0,j}[k]\mathcal{X}[k] \quad (41)$$

### Acknowledgments

This research is supported by Advanced Technology R&D Center at Mitsubishi Electric Corporation. The first author would like to acknowledge additional support from the National Science Foundation. This material is based upon work supported by the National Science Foundation Graduate Research Fellowship Program under Grant No. DGE-1650044. Any opinions, findings, and conclusions or recommendations expressed in this material are those of the author(s) and do not necessarily reflect the views of the National Science Foundation. The authors would like to thank Hao Chen and Onalli Gunasekara for their review and thoughtful suggestions for improvement. This paper is a substantially revised version of the paper AAS 18-288 presented at the AAS/AIAA Astrodynamics Specialist Conference, Snowbird, UT, August 19-23, 2018 [37].

## References

- [1] <http://en.beidou.gov.cn/>, . Accessed January 15, 2019.
- [2] <https://www.isro.gov.in/irnss-programme>, . Accessed January 15, 2019.
- [3] <http://qzss.go.jp/en/>, . Accessed January 15, 2019.
- [4] Diekelman, D., “Design guidelines for post-2000 constellations,” *Mission Design & Implementation of Satellite Constellations*, Springer, 1998, pp. 11–21.
- [5] Lee, H. W., Jakob, P. C., Ho, K., Shimizu, S., and Yoshikawa, S., “Optimization of satellite constellation deployment strategy considering uncertain areas of interest,” *Acta Astronautica*, Vol. 153, 2018, pp. 213–228.
- [6] <https://www.isac.gov.in/navigation/irnss.jsp>, . Accessed June 7, 2019.
- [7] Luders, R. D., “Satellite networks for continuous zonal coverage,” *ARS Journal*, Vol. 31, No. 2, 1961, pp. 179–184.
- [8] Lüders, R., and Ginsberg, L., “Continuous zonal coverage-a generalized analysis,” *Mechanics and Control of Flight Conference*, 1974, p. 842.
- [9] Beste, D. C., “Design of satellite constellations for optimal continuous coverage,” *IEEE Transactions on Aerospace and Electronic Systems*, , No. 3, 1978, pp. 466–473.
- [10] Rider, L., “Analytic design of satellite constellations for zonal earth coverage using inclined circular orbits,” *Journal of the Astronautical Sciences*, Vol. 34, 1986, pp. 31–64.
- [11] Walker, J. G., “Circular orbit patterns providing continuous whole earth coverage,” Tech. rep., Royal Aircraft Establishment Farnborough (United Kingdom), 1970.
- [12] Walker, J. G., “Continuous whole-earth coverage by circular-orbit satellite patterns,” Tech. rep., ROYAL AIRCRAFT ESTABLISHMENT FARNBOROUGH (UNITED KINGDOM), 1977.
- [13] Walker, J. G., “Satellite constellations,” *Journal of the British Interplanetary Society*, Vol. 37, 1984, pp. 559–572.
- [14] Ballard, A. H., “Rosette constellations of earth satellites,” *IEEE Transactions on Aerospace and Electronic Systems*, , No. 5, 1980, pp. 656–673.
- [15] Draim, J. E., “A common-period four-satellite continuous global coverage constellation,” *Journal of Guidance, Control, and Dynamics*, Vol. 10, No. 5, 1987, pp. 492–499.
- [16] Wertz, J., and for Space Technology (U.S.), N. C., *Mission Geometry: Orbit and Constellation Design and Management : Spacecraft Orbit and Attitude Systems*, Space technology library, Microcosm Press, 2001.
- [17] Mortari, D., Wilkins, M. P., and Bruccoleri, C., “The flower constellations,” *Journal of Astronautical Sciences*, Vol. 52, No. 1, 2004, pp. 107–127.

- [18] Mortari, D., and Wilkins, M. P., “Flower constellation set theory. Part I: Compatibility and phasing,” *IEEE Transactions on Aerospace and Electronic Systems*, Vol. 44, No. 3, 2008.
- [19] Wilkins, M. P., and Mortari, D., “Flower constellation set theory part ii: secondary paths and equivalency,” *IEEE Transactions on Aerospace and Electronic Systems*, Vol. 44, No. 3, 2008.
- [20] Hanson, J., Evans, M., and Turner, R., “Designing good partial coverage satellite constellations,” *Astrodynamics Conference*, 1990, p. 2901.
- [21] Ma, D.-M., and Hsu, W.-C., “Exact design of partial coverage satellite constellations over oblate earth,” *Journal of Spacecraft and Rockets*, Vol. 34, No. 1, 1997, pp. 29–35.
- [22] Pontani, M., and Teofilatto, P., “Satellite constellations for continuous and early warning observation: A correlation-based approach,” *Journal of guidance, control, and dynamics*, Vol. 30, No. 4, 2007, pp. 910–921.
- [23] Ulybyshev, Y., “Satellite constellation design for complex coverage,” *Journal of Spacecraft and Rockets*, Vol. 45, No. 4, 2008, pp. 843–849.
- [24] Crossley, W. A., and Williams, E. A., “Simulated annealing and genetic algorithm approaches for discontinuous coverage satellite constellation design,” *Engineering Optimization*, Vol. 32, No. 3, 2000, pp. 353–371.
- [25] Meziane-Tani, I., Métris, G., Lion, G., Deschamps, A., Bendimerad, F. T., and Bekhti, M., “Optimization of small satellite constellation design for continuous mutual regional coverage with multi-objective genetic algorithm,” *International Journal of Computational Intelligence Systems*, Vol. 9, No. 4, 2016, pp. 627–637.
- [26] Dutruel-Lecohier, G., and Mora, M. B., “Orion — A Constellation Mission Analysis Tool,” *Mission Design & Implementation of Satellite Constellations*, edited by J. C. van der Ha, Springer Netherlands, Dordrecht, 1998, pp. 373–393.
- [27] Wertz, J., and Larson, W. J., *Space Mission Analysis and Design*, *Space Technology Library*, Microcosm Press and Kluwer Academic Publishers, El Segundo, CA, USA., 1999.
- [28] Ulybyshev, Y., “Satellite constellation design for continuous coverage: short historical survey, current status and new solutions,” *Proceedings of Moscow Aviation Institute*, Vol. 13, No. 34, 2009, pp. 1–25.
- [29] Bruccoleri, C., “Flower Constellation Optimization and Implementation,” Ph.D. thesis, Texas AM University, 2007.
- [30] Avendaño, M. E., Davis, J. J., and Mortari, D., “The 2-D lattice theory of Flower Constellations,” *Celestial Mechanics and Dynamical Astronomy*, Vol. 116, No. 4, 2013, pp. 325–337. doi:10.1007/s10569-013-9493-8, URL <https://doi.org/10.1007/s10569-013-9493-8>.
- [31] Lutz, E., Werner, M., and Jahn, A., *Satellite systems for personal and broadband communications*, Springer Science & Business Media, 2012.



- [32] Chylla, M. A., and Eagle, C. D., “Efficient computation of satellite visibility periods,” *Spaceflight Mechanics 1992*, 1992, pp. 823–834.
- [33] Alfano, S., Negron Jr, D., and Moore, J. L., “Rapid determination of satellite visibility periods,” Tech. rep., AIR FORCE ACADEMY COLORADO SPRINGS CO, 1992.
- [34] Han, C., Gao, X., and Sun, X., “Rapid satellite-to-site visibility determination based on self-adaptive interpolation technique,” *Science China Technological Sciences*, Vol. 60, No. 2, 2017, pp. 264–270.
- [35] <http://help.agi.com/stk/>, . Accessed April 28, 2019.
- [36] Gurobi Optimization, I., “Gurobi Optimizer Reference Manual,” , 2016. URL <http://www.gurobi.com>.
- [37] Lee, H. W., Ho, K., Shimizu, S., and Yoshikawa, S., “A semi-analytical approach to satellite constellation design for regional coverage,” *AAS/AIAA Astrodynamics Specialist Conference*, 2018.